

AD \_\_\_\_\_

Award Number: DAMD17-00-C-0031

TITLE: Modeling for Military Operational Medicine Scientific and Technical Objectives

PRINCIPAL INVESTIGATOR: James H. Stuhmiller, Ph.D.  
Weixin Shen, Ph.D.  
Eugene Niu, Ph.D.

CONTRACTING ORGANIZATION: Jaycor  
San Diego, California 92121

REPORT DATE: September 2003

TYPE OF REPORT: Annual

PREPARED FOR: U.S. Army Medical Research and Materiel Command  
Fort Detrick, Maryland 21702-5012

DISTRIBUTION STATEMENT: Approved for Public Release;  
Distribution Unlimited

The views, opinions and/or findings contained in this report are those of the author(s) and should not be construed as an official Department of the Army position, policy or decision unless so designated by other documentation.

20040303 232

**REPORT DOCUMENTATION PAGE**Form Approved  
OMB No. 074-0188

Public reporting burden for this collection of information is estimated to average 1 hour per response, including the time for reviewing instructions, searching existing data sources, gathering and maintaining the data needed, and completing and reviewing this collection of information. Send comments regarding this burden estimate or any other aspect of this collection of information, including suggestions for reducing this burden to Washington Headquarters Services, Directorate for Information Operations and Reports, 1215 Jefferson Davis Highway, Suite 1204, Arlington, VA 22202-4302, and to the Office of Management and Budget, Paperwork Reduction Project (0704-0188), Washington, DC 20503

|  |   |  |   |                                  |
|--|---|--|---|----------------------------------|
| <b>1. AGENCY USE ONLY</b><br>(Leave blank)   |   | <b>2. REPORT DATE</b><br>September 2003                        | <b>3. REPORT TYPE AND DATES COVERED</b><br>Annual (7 Aug 02-6 Aug 03) |                                  |
| <b>4. TITLE AND SUBTITLE</b><br>Modeling for Military Operational Medicine Scientific and Technical Objectives   |   |  | <b>5. FUNDING NUMBERS</b><br>DAMD17-00-C-0031                         |                                  |
| <b>6. AUTHOR(S)</b><br>James H. Stuhmiller, Ph.D.<br>Weixin Shen, Ph.D.<br>Eugene Niu, Ph.D.   |   |  |   |                                  |
| <b>7. PERFORMING ORGANIZATION NAME(S) AND ADDRESS(ES)</b><br>Jaycor<br>San Diego, California 92121<br><br>E-Mail: jstuhmiller@jaycor.com   |   |  | <b>8. PERFORMING ORGANIZATION REPORT NUMBER</b>                       |                                  |
| <b>9. SPONSORING / MONITORING AGENCY NAME(S) AND ADDRESS(ES)</b><br>U.S. Army Medical Research and Materiel Command<br>Fort Detrick, Maryland 21702-5012   |   |  | <b>10. SPONSORING / MONITORING AGENCY REPORT NUMBER</b>               |                                  |
| <b>11. SUPPLEMENTARY NOTES</b><br>Original contains color plates. All DTIC reproductions will be in black and white.   |   |  |   |                                  |
| <b>12a. DISTRIBUTION / AVAILABILITY STATEMENT</b><br>Approved for Public Release; Distribution Unlimited   |   |  |   | <b>12b. DISTRIBUTION CODE</b>    |
| <b>13. ABSTRACT (Maximum 200 Words)</b><br><br>This report describes progress toward scientific and technical objectives of the Military Operational Medicine Research Program. The second year's work on developing a biomechanically-based assessment of behind body armor blunt trauma is described, including measurements of actual loads and estimated response. |   |  |   |                                  |
| <b>14. SUBJECT TERMS</b><br>Behind armor injury, blunt trauma, finite element modeling   |   |  |   | <b>15. NUMBER OF PAGES</b><br>61 |
|  |   |  |   | <b>16. PRICE CODE</b>            |
| <b>17. SECURITY CLASSIFICATION OF REPORT</b><br>Unclassified   | <b>18. SECURITY CLASSIFICATION OF THIS PAGE</b><br>Unclassified | <b>19. SECURITY CLASSIFICATION OF ABSTRACT</b><br>Unclassified | <b>20. LIMITATION OF ABSTRACT</b><br>Unlimited                        |                                  |

## FOREWORD

Opinions, interpretations, conclusions and recommendations are those of the author and are not necessarily endorsed by the U.S. Army

( ) Where copyrighted material is quoted, permission has been obtained to use such material.

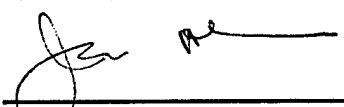
( ) Where material from documents designated for limited distribution is quoted, permission has been obtained to use the material.

( ) Citations of commercial organizations and trade names in this report do not constitute an official Department of the Army endorsement or approval of the products or services of these organizations.

( ☒ ) In conducting research using animals, the investigator(s) adhered to the "Guide for the Care and Use of Laboratory Animals," prepared by the Committee on Care and Use of Laboratory Animals of the Institute of Laboratory Animal Resources, National Research Council (NIH Publication No. 86-23, Revised 1985).

( ) For the protection of human subjects, the investigator(s) have adhered to policies of applicable Federal Law 32 CFR 219 and 45 CFR 46.

( ) In conducting research utilizing recombinant DNA technology, the investigator(s) adhered to current guidelines promulgated by the National Institutes of Health.

  
\_\_\_\_\_  
Principal Investigator's Signature

8/26/03

\_\_\_\_\_  
Date

# Executive Summary

The objective of STO-K is to produce a methodology that estimates the probability/severity of specific injuries from nonpenetrating, body armor impact and that can indicate the effects of body differences. Law enforcement and military experience, coupled with the results of previous animal studies, indicate that the injuries that occur are lung contusion, skin disruption, rib fracture, liver and spleen damage, and, more rarely, heart contusion. Previous studies of other short duration thorax loading are providing correlations of the first four injuries to local tissue stresses or local deformation. These correlations are likely to apply across species and body sizes because they are based on tissue properties, which are nearly constant across large mammal species. In blast overpressure and nonlethal weapon impact blunt trauma injury assessments, mathematical modeling has been successfully used to predict tissue stress from measurements of external loading, which in turn is used to estimate injury potential and severity. The same approach is taken in this work. First, an impact measuring device is developed that is anthropomorphically shaped, in order to properly position a ballistic garment, and that is capable of measuring the magnitude, duration, and area of the force under the armor during projectile impact. Actual projectile/armor impacts, for both hard and soft body armor, are characterized in live fire testing. A mechanical impactor is then constructed that will deliver the same, behind armor, impact to an animal in a laboratory environment. The animal studies provide confirmation of the previously observed injury modes, data on the body response, and data on injury severity. Subject-specific medical imaging, collected before each animal test, is used to build a subject-specific finite element model that is validated by the observed response data and is used to estimate the tissue stress in each target organ. From the estimated tissue stress and the observed animal injury, injury correlates are validated and refined. Finally, the methodology is extended to man by (1) using human medical imaging to construct the finite element model, and (2) modifying the tissue-based injury correlates for tissue property difference between species. The final methodology (the load measuring device, the mathematical model to compute tissue stress, and the individual injury correlates for each observed injury mode) provides a means of assessing all types of ballistic armor. By varying the anatomical features of the mathematical model, estimates of risk to a wide population can be obtained. This report summarizes the objective, approach, and progress of the work during the past year.

# Contents

|   | <u>Page</u> |
|---|-------------|
| EXECUTIVE SUMMARY .....   | ES-1        |
| <b>1. OVERVIEW .....</b>  | <b>1</b>    |
| 1.1 CURRENT METHOD OF BEHIND ARMOR ASSESSMENT .....                         | 1           |
| 1.2 PREVIOUS BEHIND ARMOR INJURY RESEARCH .....                             | 2           |
| 1.3 PREVIOUS INJURY CORRELATION RESEARCH.....                               | 7           |
| 1.4 PREVIOUS BEHIND ARMOR MODELING RESEARCH .....                           | 7           |
| 1.5 SUMMARY OF PREVIOUS RESEARCH .....                                      | 8           |
| <b>2. TECHNICAL APPROACH .....</b>  | <b>11</b>   |
| 2.1 OBJECTIVE.....  | 11          |
| 2.2 TECHNICAL APPROACH .....  | 11          |
| 2.2.1 Load Measurement Considerations .....                                 | 11          |
| 2.2.2 Body Response Considerations .....                                    | 12          |
| 2.2.3 Organ Injury Considerations .....                                     | 13          |
| 2.2.4 Response Modeling and Animal Testing.....                             | 13          |
| 2.2.5 Injury Correlation from Biomechanical Modeling and Animal Study ..... | 15          |
| 2.3 PROJECT SCHEMATIC .....   | 16          |
| <b>3. PROJECT PROGRESS.....</b>   | <b>19</b>   |
| 3.1 STO-K   19  |             |
| 3.2 ATM DEVELOPMENT, IMPACTOR DEVELOPMENT, AND LCM.....                     | 19          |
| 3.2.1 Objective, Approach, Key Issue, and Exit Criteria .....               | 19          |
| 3.2.2 Summary of Progress .....   | 20          |
| <i>ATM Prototype</i> .....  | 20          |
| <i>Live Fire Test</i> .....   | 22          |
| <i>Impactor and Launcher Development</i> .....                              | 26          |
| <i>Quantification of Impactor -- Impactor on ATM Test</i> .....             | 27          |
| <i>Numerical Model of ATM and Load Conversion Model</i> .....               | 28          |
| 3.2.3 Summary and Remaining Work .....                                      | 32          |
| 3.3 ANIMAL STUDY .....  | 33          |
| 3.3.1 Objective, Approach, Key Issue, and Exit Criteria .....               | 33          |
| 3.3.2 Summary of Progress .....   | 33          |

|   |    |
|---|----|
| <i>Animal Protocol</i> .....                                  | 33 |
| <i>Animal Testing</i> .....                                   | 34 |
| <i>Quantification of ATM Response</i> .....                   | 36 |
| 3.3.3 Summary and Remaining Work .....                        | 37 |
| 3.4 ANIMAL AND HUMAN FINITE ELEMENT MODEL .....               | 37 |
| 3.4.1 Objective, Approach, Key Issue, and Exit Criteria ..... | 37 |
| 3.4.2 Summary of Progress .....                               | 38 |
| <i>Swine Thoracic FEM</i> .....                               | 38 |
| <i>Human Thoracic FEM</i> .....                               | 41 |
| 3.4.3 Summary and Remaining Work .....                        | 41 |
| 3.5 BIOMECHANICAL CORRELATIONS FOR SIGNIFICANT INJURIES ..... | 42 |
| 3.5.1 Objective, Approach, Key Issue, and Exit Criteria ..... | 42 |
| 3.5.2 Summary of Progresses .....                             | 42 |
| <br>4. SUMMARY  | 45 |
| <br>5. REFERENCES .....                                       | 48 |

# List of Figures

|  | <u>Page</u> |
|--|-------------|
| Figure 1. Schematics of Behind Armor Blunt Trauma Research.....  | 17          |
| Figure 2. ATM Prototype (a) CAD drawing; (b) picture showing the ATM with an armor mounted; (c) Tekscan sensor and Fuji film .....                             | 21          |
| Figure 3. Force Gauge Calibration using Transfer Function Method (a) Input, output and calibrated impact forces; (b) transfer function of the force gauge..... | 22          |
| Figure 4. Behind soft body armor impact force.....   | 23          |
| Figure 5. Behind hard body armor impact force .....  | 23          |
| Figure 6. Spatial distribution of behind soft armor pressure .....   | 24          |
| Figure 7. Spatial distribution of behind hard armor pressure.....  | 24          |
| Figure 8. Pictures from live fire test.....  | 25          |
| Figure 9. Impactor and Launcher .....  | 27          |
| Figure 10. Comparison of Impactor-on-ATM measurements with live fire test results.....   | 28          |
| Figure 11. Laboratory hemisphere drop test.....  | 29          |
| Figure 12. Impact force and deformation from hemisphere drop test .....  | 29          |
| Figure 13. Hysteresis and relaxation function of the rubber .....  | 30          |
| Figure 14. FEM simulation of drop test .....   | 30          |
| Figure 15. FEM simulation of instrumented impactor on ATM. ....  | 31          |
| Figure 16. Comparison of FEM prediction and measurement at the top of rubber .....   | 32          |
| Figure 17. Comparison of FEM prediction and measurement at the bottom of rubber .....  | 32          |
| Figure 18. Some injuries observed in animal study .....  | 34          |
| Figure 19. High-speed movie snapshots of impactor-animal interaction.....  | 34          |
| Figure 20. Measurement of velocities and deformations in animal tests.....   | 35          |
| Figure 21. Measurement of impact forces and impulses in animal tests .....   | 35          |
| Figure 22. Pre- and post-impact CT imaging for Fig # 1 showed the feasibility of using medical imaging to study the soft tissue trauma injuries. ....          | 36          |
| Figure 23. Comparison of animal response and ATM response characteristics. ....  | 36          |
| Figure 24. Constructed swine anatomy and FEM of the swine thorax. ....   | 38          |
| Figure 25. FEM simulation of animal test.....  | 40          |
| Figure 26. Comparison of FEM prediction of impact forces with animal test data.....  | 40          |
| Figure 27. Comparison of FEM prediction of motion response with animal test data .....   | 40          |
| Figure 28. Human thoracic FEM.....   | 41          |
| Figure 29. Maximum rib tensile stresses and strains .....  | 43          |
| Figure 30. Lung stress predicted by FEM and the lung contusion observed in the test .....  | 44          |

# List of Tables

|   | <u>Page</u> |
|---|-------------|
| Table 1. Summary of Behind Armor Animal and Cadaver Studies. ....                     | 7           |
| Table 2. Determined Parameters for Rubber Materials .....                             | 31          |
| Table 3. Prediction of rib fracture threshold from FEM simulation of animal test..... | 43          |



# 1. Overview

## 1.1 Current Method of Behind Armor Assessment

Soldiers need effective, lightweight personal body armor (PBA) to protect them from increasingly lethal ballistic threats that can cause penetrating or blunt trauma injuries. Body armor prevents the death and severe injuries by having two functions: (1) prevent the penetration of a bullet, and (2) mitigate the blunt impact of the bullet on the body, thus prevent or reduce the blunt trauma caused by the impact. Over the past half-century, the body armor have been generally accepted as being effective in saving lives of police officers and combat soldiers. The number of police officers shot to death each year has been declining while the number of officers shot has been increasing, partly attributable to the increase in wearing bullet-resistant body armor (US Congress, OTA. 1992). In addition, the analysis of causality data of soldiers in previous combat (Sunshine 1970; Mabry *et al.* 2000), has shown that many soldiers might have been saved by the body armor.

However, the Army's body armor developers lack biomedically valid design standards and test methods to design and assess the effectiveness of new body armor systems, particularly in preventing life threatening behind armor blunt trauma injuries. As a consequence, future body armor systems may protect soldiers from penetrating injuries, yet allow serious or lethal blunt trauma injuries to occur. Or the armor may be made too heavy and uncomfortable in an attempt to protect against injuries that do not occur.

The National Institute of Justice (NIJ) (National Institute of Justice 2000) standard provides minimum performance requirements and a test method to evaluate body armor for resistance to ballistic penetration and protection from behind armor blunt trauma. In the NIJ test, a body armor sample is mounted to a plastically deforming clay backing material and subjected to a series of ballistic impacts from threat ammunition. The sample fails the test if either complete penetration occurs or the depth of the Back-face Signature (BFS) (i.e., dent in the clay) measures greater than 44 mm. The current standard has its merits in that the procedure is commonly accepted and requires minimal equipment. Also, the data shows that current armor provides good protection in actual use.

However, the validity of the Standard with respect to blunt trauma injury has been challenged because a correlation of the BFS with injury has not been established. The origin of this indentation requirement is an empirical analysis of a goat study conducted over 40 years ago and it is generally agreed that the relationship between indentation in clay and the biome-

chanical processes causing injury are unknown. Consequently, it is not known what changes in risk would occur if the indentation limit were relaxed or tightened or even what injuries are being protected against. In fact, the Standard contains the following caveat about the BFS depth measurement: *"The use of clay backing material and the subsequent BFS depth measurement does not reflect, replicate, or duplicate the physical characteristics of the human torso or its physical response to this type of stimulus."* **Furthermore, if the Standard is overly conservative, as many suspect, it could prevent the development of lightweight and effective body armor systems that could protect soldiers from current and future ballistic threats.**

The adoption of the NIJ standard has been controversial from the start. Armor manufacturers have argued that the 44 mm criterion is too stringent. It is known that PBA has been effective in preventing deaths from projectile impacts. For law enforcement, a death in officers wearing soft body armor (SBA) is so rare as to be anecdotal. Rather, death in officers not wearing SBA because it is "uncomfortable" is the issue. The body armors that pass the standard tend to be stiff and uncomfortable. There are alternative ballistic materials that are more flexible, hence more "comfortable", which can prevent penetration, but result in indentations greater than 44 mm.

Hard body armor (HBA), designed to prevent injury and death from extremely powerful projectiles, generally spreads the impact to the body over a larger area, but is still subject to the 44 mm indentation requirement. A larger diameter indentation certainly represents more impulse for the same depth and therefore the criterion may underestimate injuries related to momentum delivered. On the other hand, injuries related to the local deformation of the thorax, such as penetration and rib fracture, may be overestimated by a criterion that does not account for the area of the loading.

The current standard, due to its lack of biomechanical validation, cannot indicate what types of injuries are being prevented or minimized and what degree of safety is required. Therefore, it cannot provide guidance on whether the criterion can be relaxed and still provide enough protection. There is also no consideration on how to modify the criterion for variation in gender, size, and age of the people wearing the armor.

## **1.2 Previous Behind Armor Injury Research**

A series of studies of behind armor blunt trauma were conducted in the 1970's, which led to the current NIJ standard. Montanarelli *et al.* (1973) conducted animal tests using goats as subjects. A total of 33 goats were used. The animals were wearing the protective garments made of various plies of TL-105-26 and PED-49-IV materials and were shot by .38 caliber bullets at around 800 fps. Detailed autopsy results were collected. The observed injuries include skin

contusion, hemorrhage in subcutaneous muscles, rib fractures, and lung lesions and contusion. No cardiac injury was observed. The observed rib fractures occurred close to the impact locations. In order to compare traumatized goats with humans, the authors used an index called respiratory index, which equals the alveolar-arterial oxygen pressure difference divided by the partial pressure of oxygen in arterial blood. The index was calculated for the goat subjects from the measured arterial blood oxygen partial pressure and the venous blood oxygen partial pressure and compared with those from 177 human shock trauma patients. This index focused on the lung injury.

Goldfarb *et al.* (1975) further tested the validity of certain assumptions concerning the extrapolation of damage to the goat to damage to a human. The consequences of an impact of a .38 caliber bullet traveling at a velocity of 800 feet per second (fps) when the area of impact was covered with a 7-ply Kevlar protective garment were studied using the goats. The blunt trauma experienced was correlated with expected damage if a human had been the target based on respiratory index. It was concluded that without the garment, the mortality after a random hit with a .38 caliber bullet is between 6.9% and 25.4%. If the garment is worn, the mortality is decreased to 1% to 5%. The chance of surgery being needed when the armor is not worn is 81.5% to 100% and when the armor is worn is 7% to 10%. For thoracic injuries, 14 goats were protected by Kevlar armor and impacted at the left fifth intercostal space about 12 inches from the dorsal midline by .38 bullets of velocities around 809 fps. The goats were sacrificed at 24 hours and autopsied. Reported injuries included skin contusion and lacerations, lung contusions, and one case of rib fracture. The author attempted to establish lung injury correlation that works for both goats and humans using the respiratory index. For abdominal injuries, several impacts over liver, over stomach, and three impacts over spleen were attempted. However, specific injury data were not reported.

Several assumptions were made and tested by Goldfarb: (1) 40-50kg goat is a model typical of 70-kg man in body armor studies; (2) the damage levels of various organs will be similar in goat and human if the area of impact is equivalent and the same force is applied. The authors tested the assumptions by conducting waterjet penetration studies on goat lungs, livers, kidneys and spleens. The organs were from the same animals in the impact tests and were hit with waterjets. The depth of penetration of the waterjets into each organ is measured and compared with that of human organs, though the source of human data was not reported. The authors concluded that the collapsed lungs and spleen reacted similarly for humans and goats, and the goat kidney and liver are less resistant to trauma. The author also calculated the probability of mortality by assigning an optimistic and pessimistic mortality rate to several different areas of organ and summing them up. However, no reference was made as to what the estimation was based upon.

A similar study was reported (Soderstrom *et al.* 1978), in which goats weighing about 40 kilograms and protected by Kevlar armor were impacted by .38-caliber 158-grain bullets at a velocity of about 800 fps. Twenty-five thoracic shots were made for lung injuries. Impacts to the lungs were targeted over the lateral chest in the sixth and the seventh intercostal spaces. Observed thoracic injuries included lung contusion and rib fractures. No significant changes in arterial oxygenation or systemic blood pressure were encountered. Twenty-two impacts were made for cardiac injuries, targeted on the "cardiac window" during end expiration. One significant injury of disruption of two aortic valves was reported. Eighteen impacts over the liver aimed directly in the eleventh intercostal space produced liver contusions or singular small fractures in fourteen cases. The attempts were made to shoot the spleen directly in the eleventh intercostal space, with one leading to a contusion on the inferior edge of the spleen. Four of the eight impacts over dilated bowel resulted in perforation, whereas in 13 assaults over nondilated bowel, no perforation occurred. Typical skin wounds, behind the unpenetrated armor, consisted of an area of superficial laceration about 2 to 4 cm in diameter surrounded by an ecchymotic and erythematous area. Laceration also occurred occasionally extending into the underlying thoracic and abdominal wall muscles.

Metker *et al.* (1978a) also used goats as subjects and studied the cardiac injuries that might be caused by behind armor impacts. Twenty-five anesthetized Texan Angora goats weighing 36.8 kg to 77.4 kg were protected by 7 plies of Kevlar 29. Twenty-two animals were impacted with a standard .38-caliber 158-grain bullet. One animal was impacted with a standard .45-caliber 234-grain bullet. The impact location was directly over the myocardium. Extensive cardiac monitoring was performed including cardiac output, EKG, left ventricular end diastolic pressure, systolic blood pressure, and serum CPK and LDH. The study produced small myocardial contusions, damage to the valvular structures (aortic valve disruption), and great vessel injury (aortic laceration).

An extension of the goat tests to using surrogate materials was studied by Metker *et al.* (1975b) and Prather *et al.* (1977). Metker *et al.* attempted to measure the 'backface signature' of flexible armor materials struck by .22-caliber and .38-caliber bullets using high-speed photography of backlighted gelatin blocks. Several layers of Kevlar or denier material were placed and fastened in front of the gelatin block and shot by either .22 or .38 caliber bullets. The backface deformation was measured by high-speed camera systems (up to 4000 fps) and digitized. The peak deformation profile was fit by parabolic equation as  $y^2 = cx+a$ . The author also used a discrete parameter model to establish the discriminating lines of zones of live/die criteria. The model involves parameters such as mass of deformed armor, effective armor velocity, etc. They mentioned that the live/die criteria was based on animal test data, but no details were available in the report.

Prather *et al.*, on the other hand, used several backing materials for assessing blunt trauma from behind armor blunt impact. The materials tested included 20% gelatin; an oil-based modeling clay called Roma Plastilina; and one kind of foam. V50 ballistic limit tests were conducted on the various materials covered by 7 plies of Kevlar 29 and 8 plies of Hi-Tenacity Nylon. The projectile used was the 0.22-caliber 40-grain lead bullet. Deformation tests were also conducted to obtain the deformation-time history of armor over various materials impacted by a 200-gram 80-millimeter hemispherical missile at approximately 55 meters per second. The authors concluded that the depth of deformation from clay was closest to human thorax, though the reference to human thorax response data was not provided. And the peak deformation was reached in a shorter time frame from clay than on human. The author also related the depth of deformation on clay backing to lethality calculated from the equation:  $\ln(MV^2/W^{1/3}DT) < 9.2$ , where M is the projectile mass in grams; V is the projectile velocity in meters per second; W is the body weight in kilograms; T is the tissue thickness in centimeters; and D is the projectile diameter in centimeters. The mass of projectile also had to be adjusted to include the deformed portion of the armor.

Several NATO countries conducted live animal tests in Oksbol, Denmark in March 2000. The study examines characteristics of behind body armor blunt trauma produced by high velocity, low mass projectiles in an animal (swine) model (Sarron *et al.* 2000a; Sarron *et al.* 2000b). In the trial, 27 animals were randomly assigned to one of four groups, Group 1 (n=8), Group 2 (n=8), Group 3 (n=8) and Group 4 (Control) (n=3). The weight of the pigs was 60 kilograms ( $57 \pm 4$  kg). 7.62 mm NATO bullets fired by a fixed barrel mounting was used through the trial. Three configurations of armor protection were used. Pigs in Group I were protected by a UK-manufactured ceramic plate (Plate G1, 2 peak plate). Pigs in Group II were protected by the same plate with foam backing along its outer rim. Pigs in Group III were protected by a UK-manufactured ceramic plate (Plate C, 1 peak plate) that was thicker. Plate G1 was expected to produce a characteristic double peak pressure tracing when hit by a 7.62 mm projectile. Two accelerometers, A1, A2, and three pressure sensors, P10, P12, P2, measured the accelerations and pressures at selected locations inside the animal and on the armor plate. Important physiological responses are also measured during the tests. Heart rate and respiration rate decreased immediately after impact and returned to a normal baseline when no difference among different armor was observed. Injuries were observed at five minutes after impact and recorded during postmortem. The observed injuries included skin lesions, lung contusions, rib fractures and a very limited number of heart injuries. Lung contusion was the leading cause of major injuries. It was estimated that all injuries had an AIS score of 2 or 3 (serious, nonlife-threatening) because of lung contusion. Different injury ranking indexes were also tried. A detailed analysis was conducted by Shen (2001) for all the acceleration and

pressure measurements with quality of the data examined for each test and questionable test data discarded. Frequency analysis was performed for the acceptable data. It was concluded that in-animal accelerations and pressures were sensitive to the mounting of the sensors and sensor orientation, which is difficult to control in testing. The sensors were also very likely to be damaged and measurements were unreliable. The animal trial did provide a qualitative description of the behind armor impact event. The phases and duration of impact as well as the size of impacted area were estimated. It was suggested that a measurement device that can reliably measure the duration and extent of the behind armor impact force should be developed.

Haley *et al.* (1996) of Army Aeromedical Research Laboratory (USAARL) attempted to determine the Kevlar(tm)-to-chest space (standoff) needed to prevent such BBA injury and/or incapacitation by conducting a live fire test series on 12 man-size pigs wearing chest armor with polyvinyl chloride (PVC) standoff foam of 0.55, 0.82, and 1.07-inch thickness. The BBA impact forces were measured by using multiple miniature force gauges between the armor and the pig.

Kamenev *et al.* (2000) conducted animal tests using 80 mixed-breed dogs with an average body weight of 16-20 kg. The dogs were protected by commercial rigid body armor made in Russia and impacted with a 12-caliber hunting rifle with varying levels of impact loads controlled by the power charge of the cartridges and the thickness of shock-absorbing pads placed behind the armor plates. Blunt trauma was inflicted on the dogs in the region of the left cardiac ventricle, the lungs, the liver, spleen and the center of the abdomen. The author measured the impact loading in terms of the acceleration created by the impact. For thoracic impacts, the most striking injury is lung contusion and hemorrhage in the zone of direct impact and secondary to the impact. A limited number of rib fractures and cardiac injuries were also reported. For abdominal impacts, liver and spleen lacerations were reported to occur secondarily when the point of impact was located distally to such organs. The author established the tolerance of individual organs and impact areas of the dog subjects to impact load in terms of the acceleration.

DiMaio *et al.* conducted human cadaver tests at Armed Forces Institute of Pathology to study the response of the thorax. According to Jolly (2000), cadavers were protected by a bullet-proof vest incorporating either soft armor alone or soft armor plus one of the two variations on a ceramic plate. Cadavers were struck with either a NATO 9mm round or a NATO 7.62mm M80 ball round fired from a distance of 50 feet. Accelerations of the sternum, spine, and carina, and the left and right ventricular pressures were recorded. Post-shot autopsies were performed to judge injury and assess survivability. However, no actual test data have been reported. A summary of animal and cadaver studies is given in Table 1.

**Table 1. Summary of Behind Armor Animal and Cadaver Studies.**

| Source              | Target           | Armor                 | Projectile            | Location          | Major Injuries   | Response                                     |
|---------------------|------------------|-----------------------|-----------------------|-------------------|--|--|
| Goat Test           | Goat             | Nylon<br>Kevlar<br>29 | .22 .38<br>bullets    | Thorax<br>Abdomen | Lung contusion<br>rib fracture<br>cardiac injuries<br>Liver & spleen<br>injuries | No   |
| NATO Test           | Swine            | Hard<br>Armor         | 7.62 mm<br>Nato rifle | Thorax            | Lung contusion<br>rib fracture<br>cardiac injuries                               | Acceleration<br>and<br>pressure in<br>animal |
| Russian Dog<br>Test | Dog              | Hard<br>Armor         | Hunting<br>rifle      | Thorax<br>Abdomen | Lung contusion<br>rib fracture<br>cardiac injuries<br>Liver & spleen<br>injuries | Acceleration<br>of Plate                     |
| USAARL              | Swine            | Hard<br>Armor         | .50<br>Caliber        | Thorax<br>Abdomen | Lung contusion<br>Heart lesion   | BBA force<br>Acce. On<br>plate               |
| Dimaio              | Human<br>Cadaver | Kevlar                |                       |                   |  |  |

### 1.3 Previous Injury Correlation Research

The following list of injuries can be anticipated from BBA trauma.

- ? Lung Contusion
- ? Rib Fracture
- ? Liver Laceration
- ? Skin Penetration and Contusion
- ? Heart Lesion

For other ballistic applications, correlations of injury with local tissue stress or local deformation are being developed for lung contusion, rib fracture, liver laceration, and skin penetration and contusion. Only heart lesions do not have a tissue-based correlate to use as a starting point for the current project.

### 1.4 Previous Behind Armor Modeling Research

Only two efforts to model thoracic response to behind armor impact have been reported. Hughes (1999) and Jolly *et al.* (2000) developed a simple finite element model of human thorax to simulate the response of human skeletal response, in terms of acceleration, to the ballistic impact on body armors. The model was intended to calculate only motion response. Since no

organ was incorporated, it lacks the capability of predicting stress that can be directly related to injuries. In addition, no detailed information was provided on how material model and parameters were determined. The mesh used in the calculation appeared too rough and no mesh study was conducted.

## 1.5 Summary of Previous Research

The preceding review of previous research leads us to the following conclusions. These conclusions form the basis for our research approach.

There is a lack of specific, human injury data to form correlations. Because the armor that passes the current standard has performed so well, there have been relatively few non-penetrating injuries in field use. Even when field data exists, the impact conditions (speed of projectile, angle of impact, etc.) are usually not known. Because of the violent and potentially lethal consequences of live fire testing, no systematic human exposure testing will be ethically allowed.

The nature of observed injuries requires live test subjects. Although human data from the field is sparse, these limited data plus the animal tests that have been conducted suggest that the primary injuries are: skin disruption, lung contusion, heart contusion, liver laceration, and rib fracture. The first four injuries require viable organs or tissues in order to occur. Although rib fracture occurs in cadaver test subjects, those subjects are usually elderly and without a viable musculature, so there is uncertainty about the relevance to rib fracture in live, healthy, young subjects. Along with the political sensitivity considerations, cadaver testing will not provide the injury data required.

Animal testing introduces anatomical complications. Large mammals, especially the farm animals sheep, pig, and goat, have been the test subjects for nearly all impact trauma studies conducted. Data from these animals have provided most of the blunt trauma criteria, including the current body armor standard. The differences in body mass, organ size and placement, and overall anatomical features, however, complicate translating injury relationships to man if those relationships are based on external deformation of the body.

Organ/Tissue properties and injuries are similar across all large mammal species. Although organ placement and size vary across species and individuals within species, the functions, relationships, and material properties of these tissues are remarkably uniform. Lung, liver, skin and bone have been shown to have similar mechanical properties and similar damage limits, when expressed in terms of local stress or strain. Although some differences remain, injury correlations based on tissue stress or strain are likely to be valid across species and body sizes.



In vivo measurements of tissue stress or strain are not practical options. A correlate of tissue damage to tissue stress/strain will require estimates of the tissue response to impact to go along with the observed damage. *In vivo* placement of such gauges is not practical and cannot be done without the potential for artifact. Even relatively noninvasive measurements of rib acceleration are difficult to implant and often lead to hard to interpret results. Measurements of intrathoracic pressures have been made in blast studies, but the instruments cannot be placed far enough peripherally in the lung to be in a damage region and involve considerable surgical skill and expenses. Furthermore, the instruments often fail during the violent loading.

Finite Element Modeling (FEM) provides a means to estimate tissue stress/strain under impact conditions. Current FEM technology, coupled with high-resolution medical imaging, can produce computational models that adequately resolve internal organs and compute the distribution of stress and strain. A FEM of the thorax response to blast loading has produced estimates of lung stresses that can be correlated with observed lung contusion. That model has produced equally encouraging results when studying lung contusion from nonlethal weapon impacts. We expect the same modeling approach to extend to BBA lung contusion. We also expect FEM to be able to translate thoracic deformation into accurate estimates of stress and strain in the ribs. Another FEM, developed for nonlethal weapon impact, has shown that skin penetration injury can be cast in an injury-tissue stress form that is valid across species. We would expect similar results for liver laceration. Consequently, we plan to use finite element modeling to provide body deformation and subsequent tissue response under BBA loading and that the tissue stresses estimated in this manner can be used to build biomechanical correlates of injury.

To ensure that the injury results are appropriate to BBA trauma, the animal tests must be conducted with an impact that closely matches that felt behind body armor for actual projectiles and armor. Since weapon firing will not be allowed in any laboratory environment, it is necessary to build an impactor that produces the same force distribution on the body surface as the body would see behind armor. A free flying impactor will be developed that, upon impact with the body, will produce a force distribution, in space and time, similar to BBA impact. The validity of this impactor will be directly confirmed by demonstrating that it produces the same force distribution as the projectile-armor combination.

Calibration and validation of a thoracic FEM requires thoracic response data under BBA loading conditions. Since there will not be tissue stress data to validate the FEM predictions directly, the accuracy of those predictions will have to be judged based on the fidelity of related quantities. First, we plan to reproduce the anatomical details of the test subject, by generating an FEM grid based on high-resolution medical imaging taken before the exposure. Second, we

plan to use tissue material properties based as closely as possible on independently reported values. Third, we plan to simulate the impactor in the simulations of the animal tests, giving it the initial velocity, direction, and point of impact in the test. The validity of the FEM will be judged by the accuracy to which the thoracic response, measured by the dynamics of the impactor after impact, can be reproduced.

These considerations lead us to adopt a technical approach of: (1) measuring and estimating BBA impact force; (2) using mathematical modeling to predict body response and tissue stress; (3) establishing correlations between tissue stress and injury; and (4) using animal testing to validate the body response model and injury correlations. The approach recognizes that, BBA impact force, including its magnitude, duration and spatial distribution, is the key indication of how well the armor performs and protects the body. The plan recognizes that injury, identified as structural and morphological changes that prevent the tissues from performing its normal physiological and structural functions, occurs when stresses exceed the level that the tissues can comfortably sustain. Finally, the plan recognizes that animal testing, under loading closely matching behind armor loading, will be required to provide the data necessary to validate the mathematical models and validate the injury criteria.

## 2. Technical Approach

### 2.1 Objective

The objective of STO-K research is to produce a criterion for nonpenetrating, behind body armor (BBA) impact that estimates the probability and severity of specific injuries and that can indicate the effects of body differences, based on a practical measurement technique.

### 2.2 Technical Approach

The technical approach adopted involves four steps: (1) measuring and estimating BBA impact force; (2) using mathematical modeling to predict body response and tissue stress; (3) establishing correlations between tissue stress and injury; and (4) using animal testing to validate the body response model and injury correlations. The approach recognizes that BBA impact force, including its magnitude, duration and spatial distribution, is the key indication of how well the armor performs and protects the body. The plan recognizes that injury, identified as structural and morphological changes that prevent the tissues from performing its normal physiological and structural functions, occurs when stresses exceed the level that the tissues can comfortably sustain. Finally, the plan recognizes that animal testing, under loading closely matching behind armor loading, will be required to provide the data necessary to validate the mathematical models and validate the injury criteria.

#### 2.2.1 Load Measurement Considerations

Soft body armor works by catching the bullet in a web of strong fibers. The load mitigation component of soft armor, the ballistic panel, is made from multiple layers of weaved ballistic fiber. The ballistic fiber, Nylon, Kevlar, or Spectra, is very strong and has a high modulus and strength-to-weight ratio compared with natural fibers. When the bullet strikes the fiber, a longitudinal strain wave forms and propagates along the fiber to pull the material toward the impact location. This longitudinal wave speed is very fast due to the large modulus of the material. A transverse wave is also formed and deforms in the direction of impact. The speed of this transverse wave, which is determined by the longitudinal wave speed as well as the magnitude of strain at the wave front, is usually one order smaller than the longitudinal wave speed. Therefore a V-shaped deformation results for each fiber and a conical deformation of the fabric sheet (Vinson *et al.* 1975). Cunniff (1992) gives a detailed description of deformation patterns of the ballistic fabrics. During the deformation process, materials away from the impact

location and successive layers of material are excited. The momentum of the bullet is transferred to the fabric and the body over a much larger area than the size of the bullet, thus preventing the penetration of the bullet. Bullet kinetic energy is also dissipated through the plastic deformation or fragmentation of the bullet, the plastic deformation or the breaking of the fibers, as well as friction.

While soft body armor is able to stop pistol bullets, it cannot stop rifle bullets that have higher velocities and carry much higher kinetic energy. Hard armor that combines the soft armor with a ceramic or steel ballistic plate has to be used. Under high-speed impact, most ceramics pulverize (Rajendran 1993). It can dissipate a significant amount of energy through inelastic deformations due to micro-cracking and dislocation generated micro-plastic flows. A pulverized zone much larger than the bullet size is formed in the ceramic plate. The bullet also tends to be fragmented completely. Therefore, a significant amount of the energy of the bullet is dissipated and the momentum of the bullet is spread to a large area, where it is further reduced by the deformation of the ballistic fibers in the soft armor.

The load measuring device, therefore, must accurately measure the behind armor impact characteristics. The behind armor impact will be characterized in terms of the impact force duration, magnitude, and area. To be able to conduct representative animal tests, the impactor used in the laboratory must be able to recreate these same force characteristics.

### **2.2.2 *Body Response Considerations***

During the BBA impact, the body surface deforms under the BBA loading. This surface deformation, in turn, leads to the deformation of tissues that are not in contact with the armor and the propagation of the stresses and strains throughout the body. The rate, magnitude, and localization of these internal stresses depend on the material properties of the body components and the characteristics of the loading itself. Injuries of organs occur only when the tissue stresses exceed the tissue strength.

Body response dynamics can be characterized in three ways: (1) the impact force, (2) the local deformation at or near the impact location, and (3) the stress inside the tissue. The impact force depends on both the characteristics of the impacting object and of the body being impacted. Because the impact surface deforms, it is difficult to measure the force directly. For a rigid impactor, however, the impact force can be inferred from the acceleration of the impactor. Deformation at the impact location is also difficult to measure, but, again, in the case of a rigid impactor, the deformation can be inferred from the shape of the impactor and its linear motion. These two measures of body response, because they are practical to measure directly for a rigid impactor, are usually used to characterize the surface response of the body. Unfortunately, they

are not mechanically related to organ stress and therefore have not produced correlates that are valid over a wide range of impact conditions.

Stress in tissue is very difficult to measure directly, *in vivo*, during impact conditions, so there is virtually no tissue stress data available, and it is not practical to collect such tissue stress data in this project. Tissue stress can be calculated from numerical models, such as a finite element model, from measured impact force when the anatomy and material properties are estimated. We shall adopt this approach. The impact force and surface deformation, which can only be predicted correctly if the complete structural description is correct, will be used to assess the validity of the mathematical model.

### ***2.2.3 Organ Injury Considerations***

Both the stress developed in the tissues and the strength of tissues are affected by the velocity, duration, and area of the BBA impact. Lung injury is velocity related since the effective impact velocity from the BBA impact can exceed the acoustic speed of lung material, which is on the order of 30 mps. Supersonic shock waves form and lead to the concentration of energy and stress in a thin layer of shock-wave front. This leads to a high potential of injury. Therefore, it is no surprise that lung contusion is one of the major injuries observed.

For other types of injuries such as rib fracture, liver laceration, etc, the tissue material moves at a speed lower than the acoustic speed, while stress waves move in the body at sound speed and the actual stress distribution is the result of stress wave propagation, reflection, refraction, and interference due to the complexity of anatomical geometry. The rib fractures during BBA impact tend to occur directly underneath the impact location, while rib fractures in automobile accidents tend to occur away from the impact location. This is due to the factor that BBA impact is faster and more concentrated, which will lead to higher stress underneath the impact location; while the slower but larger impact tends to lead to higher stress away from the impact location due to the deformation of the ribs.

The loading speed also affects the stress due to the viscosity of most biotissues and the magnitude of stress depends not only on the magnitude of the load but also on the rate of loading. On the other hand, the strength of material expressed by a tolerable stress is also affected by the rate of loading as well as the loading condition. Therefore, it is crucial to understand the loading rate and condition for analyzing response or injury test data and for developing a model to predict body response.

### ***2.2.4 Response Modeling and Animal Testing***

Since human tests that may lead to injury are not possible due to obvious reasons, there are primarily four kinds of tests that can produce response measurement: human volunteer

tests that will not cause injury; human cadaver tests; animal tests; and surrogate tests. Noninjurious human tests can provide impact responses of real, live humans, however, these response are usually quite different from the injury level response and are only of limited value. The cadaver has the advantage of having the real anatomy and material of a human. But there are also several significant disadvantages. First, a cadaver is a dead person; therefore, most types of injuries cannot be measured, except for bone fracture. Physiological changes to injury cannot be studied. Second, due to practical reasons, cadavers tend to be old and the number of cadavers that can be used in a test is usually limited, therefore the responses from a cadaver may not be representative of the general population. Third, the material properties of cadaver tissue may be quite different from living tissue; this also affects the validity of the measured response data. Animal tests can overcome many of these limitations, however, functional and anatomical differences between human and animal subjects have to be considered. And the response data may not be directly extrapolated for humans. Both animal tests and cadaver tests are usually difficult to conduct. Surrogate tests measure responses from a surrogate device such as a dummy, which is assumed to respond like a human. Obviously, a surrogate test cannot provide information on injury and physiological responses. In addition, due to the complexity of a human body, a surrogate cannot completely and accurately reproduce all the human responses. It can only be used in the cases where loading conditions are well defined and response data have been well studied. The response data from surrogate studies cannot be generalized without careful validation. The real value of surrogate tests lies in providing the information of impact characteristics such as impact force and energy and in the relative easiness of conducting the tests.

A biomechanical model that is based on the fundamental laws of physics and calibrated against the animal or cadaver tests has a much greater range of applicability than a surrogate that targets a specific type of injury under a very specific impact condition. Model simulations are much easier and less expensive than surrogate testing and population variation can be included. More importantly, biomechanical models have the capability to predict stress that is directly related to injury. Calibrated injury correlations based on stress are more fundamental and can be used for impact conditions that are different from the tests. Boundary conditions including the impact forces have to be provided in order to drive the model simulation.

One of the most commonly used models is the finite element model, which has the capability of accurately representing the anatomy of the subject. The development of a highly accurate model, however, is a challenging task. The anatomy of humans or animals is complex. The material characterization of tissue is difficult. Tissues are usually highly nonlinear and their response is rate dependent. Constitutive relationships that describe the tissues tend to have a large number of parameters that cannot be easily determined from a laboratory test. In addition,

boundary conditions (impact conditions) are needed to drive the model, which has to be from test measurements.

The approach adopted here in dealing with the BBA problem is to develop the biomechanical animal model in conjunction with controlled animal tests. High-resolution medical images provide the accurate geometry to build a model; material parameters obtained in the literature can be used as baseline values; instrumented impactor impacts the animal and provides impact force and chest wall deformation and velocity at the impact spot; and numerical simulations are conducted by varying parameters until the simulation produces the same impact force and chest wall deformation as measured.

A human biomechanical model can then be developed for accurately predicting the human responses due to behind armor impact that is characterized by using the surrogate test device. The model should not only predict the gross motion of the body, it should also predict the stress in the rib, lungs, heart, liver, kidney, spleen and other organs where injuries are concerned.

#### ***2.2.5 Injury Correlation from Biomechanical Modeling and Animal Study***

There are several sources for the injury data: human injury, animal studies, and cadaver studies. Human injury data from traumatic events and the subsequent clinical diagnosis is important to obtain the epidemiology of different injuries and understand the mechanisms leading to the injuries. It is usually not adequate to determine the threshold or correlation of injury, since in almost all the cases involving blunt trauma, loading condition or response data is unavailable. Cadaver testing can only produce bone fracture. Also, because cadavers tend to be old and number of cadavers that can be used in a test is usually limited, the injury data may not be representative of general population. Therefore, the best injury data for developing injury tolerance or correlation is the data from animal tests. However, special attention has to be paid to account for the anatomical and structural differences between humans and animals.

The method used here is to use the biomechanical animal model and animal study to establish the injury correlation or threshold for individual injury modes. The injury correlation will be extrapolated to humans. The biomechanical animal model, developed using the real anatomy of the animal subject and calibrated against the impact force and chest wall motion, will predict the stress distribution in major organs such as lungs, heart, ribs, liver, etc. The stress predictions will be compared with the injury data measured during the test. By conducting a series of animal tests to create different levels of injury, the correlation between stress and injury potential can be established.

The correlation developed in this way involves only the tissue material property and strength. Therefore, the concern of anatomical differences in extrapolating animal data to human can then be resolved by using a biomechanical human model to predict human response. This approach also addresses the issue of varying tissue properties with species, age, and many other factors by allowing them to be included. Tremendous knowledge of lung injury and material properties for both human and animal lungs have been obtained through previous research on blast injury and blunt trauma (Elsayed 1997; Yen *et al.* 1988; Johnson *et al.* 1986; Fung *et al.* 1988; Fung *et al.* 1985; Cooper *et al.* 1991; Goncharoff *et al.* 1989; Pode *et al.* 1989; Suneson *et al.* 1989 ). A large number of data for both animal and human bones is also available (Miller-Young *et al.* 2002; Behiri *et al.* 1984; Gottesman *et al.* 1980; Reilly *et al.* 1975a; Pope *et al.* 1974; Reilly *et al.* 1975b; Reilly *et al.* 2000; Currey 1979; Currey 1990; Gunaratne *et al.* 2002). There is also research that studied the tolerance to impact for human and animal organs (Goldfarb *et al.* 1975). However, it is recognized that the lack of tissue property data obtained in the similar loading rate as in BBA impacts may be a concern. But this is an issue that is unlikely to be addressed within the budgetary and time constraints of the STO-K project.

## 2.3 Project Schematic

Figure 1 gives a schematic view of the research approach. The research is separated into four major elements. The first element deals with the measurement and interpretation of the BBA impact load. It will develop and calibrate an Anthropomorphic Testing Module (ATM) that is rugged enough to withstand a ballistic impact, able to accommodate a ballistic garment, and measures both the temporal and the spatial distribution of impact forces. Live fire tests will be conducted using the ATM. A Load Conversion Model (LCM) that determines the impact parameters from the ATM measurements will also be developed.

The second element focuses on the animal testing. Instrumented impactors and a launching device that can be used to simulate behind armor impacts will be developed and applied to animal subjects to reproduce significant injuries from BBA trauma. The animal study will collect geometrical data from medical imaging, response data, and injury data, for the development of response model and injury correlations.

The third element involves developing both swine and human finite element models that can be used to predict response. The animal models will be based on medical images taken in the animal studies. The models will be calibrated against the measured animal response data. A human model will be based on available medical images of human beings.



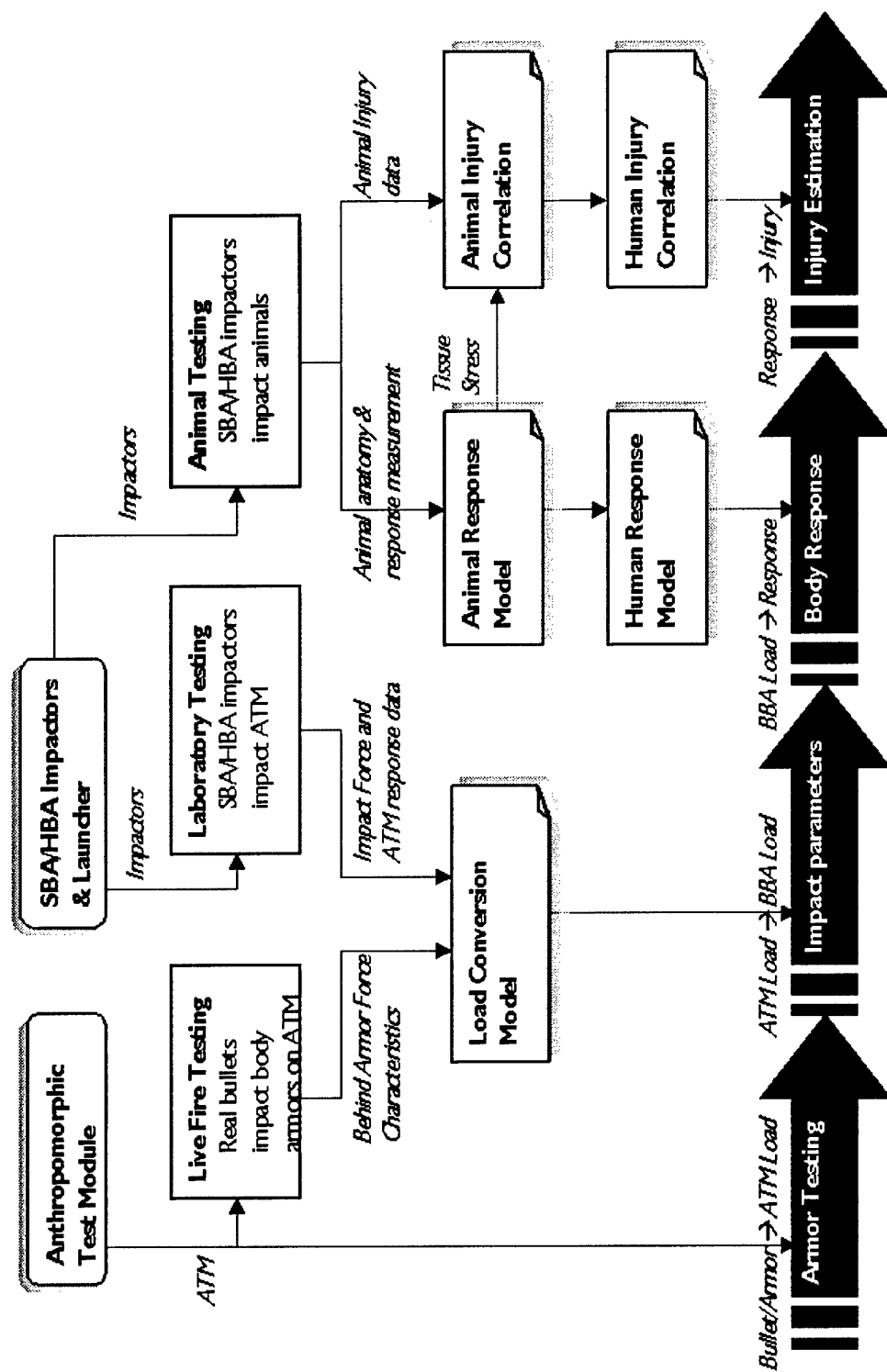


Figure 1. Schematics of Behind Armor Blunt Trauma Research

The last element develops the injury correlations based on model simulations and animal test data. The calibrated animal finite element model will be used to simulate the animal tests and predict the stress distribution in animal organs. Based on the comparison of observed injury pattern and data with the calculations, injury correlations can be developed. These correlations will then be extrapolated to humans.

Figure 1 also demonstrates how the outcome of the research is to be used in the final BBA injury methodology. The ultimate product includes an ATM and a software package that is made up of a load conversion model, a human response model, and an injury assessment model. Armor being tested is mounted on the ATM and hit by a real bullet. The load conversion model provides BBA impact force characteristics by interpreting the ATM measurement. Simulations using the human response model driven by the impact force characteristics calculate the major body responses to the BBA impact, and ultimately, potential for different kinds of injuries is estimated from the injury assessment model based on the calculated response values.

### 3. Project Progress

This section summarizes the objective, technical approach, key issues, exit criteria, and progress in the four elements of the research project as well as the whole project.

#### 3.1 STO-K

The objective of STO-K is to produce a criterion for nonpenetrating, behind body armor impacts that estimates the probability and severity of specific injuries and that can indicate the effects of body differences, based on a practical measurement technique.

The STO-K is separated into four major elements:

- ? Developing ATM to measure BBA load
- ? Animal study to provide response and injury data
- ? Animal and Human Finite Element Model
- ? Development of biomechanical correlations for significant injuries

The testing device and injury criteria developed from STO-K can be judged in light of the following:

- ? The degree that the observed injury in animal tests can be correlated with the prediction of the biomechanical model, when driven by the load measured by the ATM
- ? The reasonableness of the predictions for currently used armors
- ? The plausibility of the criterion's prediction of variation of risk with varying parameters such as body mass, etc.
- ? Reenactment: validate against the data of body armor in use.

#### 3.2 ATM Development, Impactor Development, and LCM

##### 3.2.1 *Objective, Approach, Key Issue, and Exit Criteria*

The objectives of this task area include: (1) to develop a test instrument rugged enough to withstand ballistic impact, can accommodate ballistic garments, and estimates the load distribution in time and space; (2) develop an impactor that can be instrumented and reproduce the BBA impact force characteristics; (3) a load conversion model (LCM) that can interpret the

measurements from ATM and convert them into parameters that can be input into the mathematical response model.

Despite some efforts (Haley *et al.* 1996; Sarron *et al.* 2000a) to measure BBA impact force on animals, direct measurement of the BBA impact force is difficult. Due to the proximity to the ballistic impact, pressure sensors, accelerometers, and force, gauges tend to fail or provide incorrect measurements (Shen 2001). The approach used here is to obtain the BBA impact characteristics in two steps:

- 1) Develop a surrogate device (ATM) that measures the force characteristics behind surrogate materials, which is much easier than the direct measurement of BBA load; and
- 2) Develop a method to estimate the BBA loading characteristics based on the ATM measurements.

Requirements of the ATM include:

- ? ATM should be durable. The test device has to withstand a significant number of ballistics impacts and still provide reliable measurements.
- ? Bullet-armor-ATM interaction has to be similar to bullet-armor-body interaction. Armor has to function and damage in a similar fashion.
- ? The ATM measurement must be able to be used to estimate and differentiate the BBA impact characteristics, judged by the magnitude, duration of the overall momentum delivered, and the area of impact.

Regarding the development of impact, the key issues to be addressed include:

- ? The impactor has to deliver a load similar to the BBA impacts, in terms of the impact magnitude, duration and area
- ? The sensor instrumented on the impactor has to survive the impact against the animal and give accurate measurements

### **3.2.2 Summary of Progress**

#### **ATM Prototype**

An ATM prototype was developed and is shown in Figure 2. An articulated system that can incorporate an anthropomorphic model frame is attached to a rigid backing. An armor vest can be easily mounted onto the frame, providing a realistic imitation of a real person wearing an armor vest. The articulated system allows the easy position of the impact spot during testing.

A *force gauge* is rigidly mounted on the rigid backing underneath the rubber. The force gauge measures the total behind armor force-time history. A *high-speed Tekscan sensor* (10 kHz sampling rate) is also placed on top of the force gauge to measure the temporal distribution of the force. Two layers of rubber (soft rubber and neoprene rubber) are placed over the force gauge to serve as padding between the armor and the gauge. The force gauge, the Tekscan sensor, and possibly a *high-speed camera*, will be connected to a synchronizer and computers to collect data. The Pressurex tactile pressure measuring films (Fuji films), which measures the maximum spatial distribution, can also be placed over the force gauge, between the rubber, and directly behind armor.

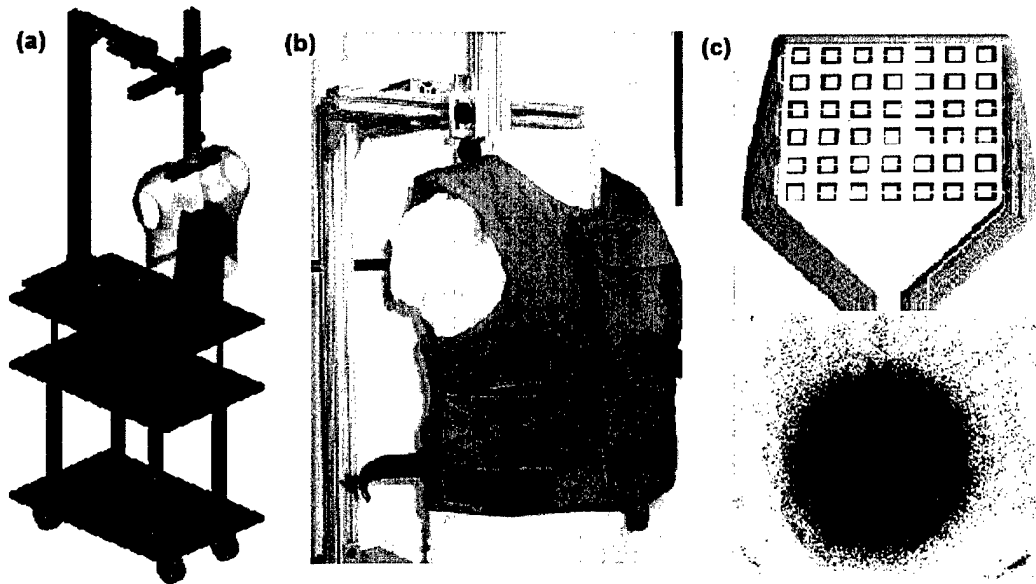


Figure 2. ATM Prototype (a) CAD drawing; (b) picture showing the ATM with an armor mounted; (c) Tekscan sensor and Fuji film

The force gauge was calibrated using a transfer function method. First, a given impact force  $F_i(t)$  is applied onto the force gauge using a standard laboratory force hammer. The impact force is measured by the force gauge as  $F_o(t)$ . The transfer function of the force gauge can be calculated as

$$H(\omega) = \frac{F_o(\omega)F_i(\omega)^*}{F_i(\omega)F_i(\omega)^*}$$

where  $F_i(\omega)$  and  $F_o(\omega)$  are the Fourier transformation of  $F_i(t)$  and  $F_o(t)$  respectively.  $H(\omega)$  is a complex function, with the real part indicating the difference in the magnitude of frequency response of output and input signals and the complex part indicating the phase shifting of the signals. Next, the impulse response function can then be calculated from the inverse Fourier

transfer of  $H(\omega)$  as  $h(t) = \mathcal{F}^{-1}\{H(\omega)\}$ . And finally, the force gauge measurement is calibrated using the following convolution equation

$$F_o^{calibrate}(t) = \int_{-\infty}^{\infty} h(\tau) F_o(t - \tau) d\tau$$

Figure 3 shows the calibration of the force gauge installed on the ATM. The dotted and the solid lines in Figure 3a indicate the input impact force and force gauge measurement respectively. They match very well in both timing and magnitude, suggesting that the force gauge measurement is accurate. The gauge oscillates after the impact. The transfer function is given in Figure 3b. The calibrated force gauge measurement is shown as the dashed line in Figure 3a, which matches the input impact signal very well and has little oscillation after the impact.

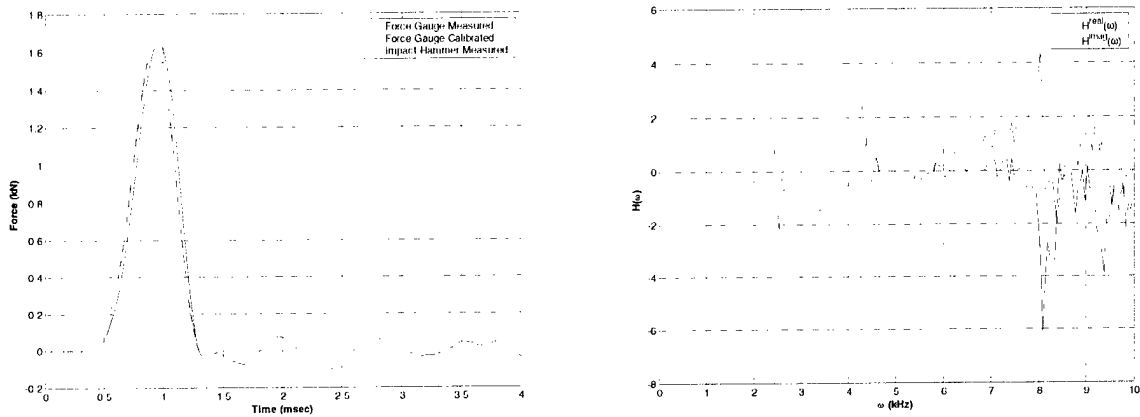


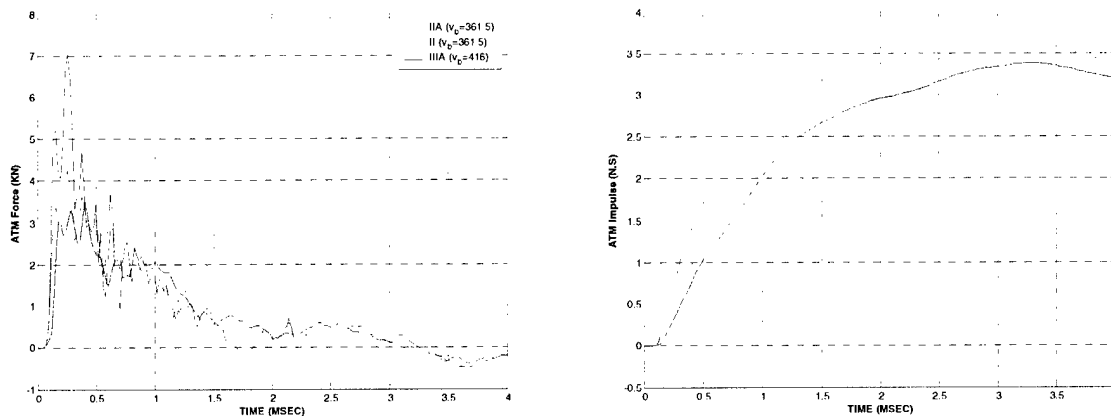
**Figure 3. Force Gauge Calibration using Transfer Function Method (a) Input, output and calibrated impact forces; (b) transfer function of the force gauge**

The same method is also used to calibrate the high-speed Tekscan sensors. Since a Tekscan sensor is made up of 42 individual sensels functioning as individual force sensors, each sensel has to be calibrated separately.

### Live Fire Test

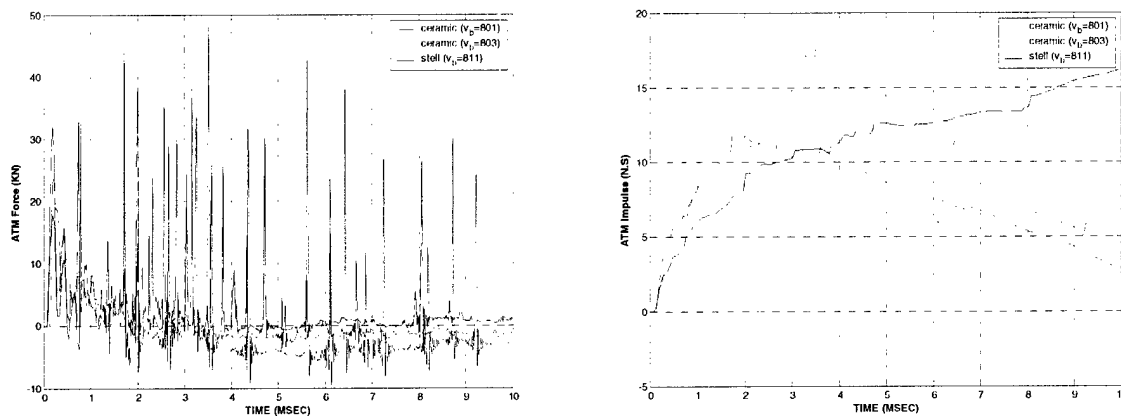
Live fire tests using the ATM were conducted. Twenty-two tests used NIJ level IIA, II, and IIIA soft body armors that were commercially purchased. Three tests used NIJ level III hard armors, including two ceramic armors and one steel armor. Force gauge, high-speed Tekscan sensor, and Fuji-films placed behind armor, between rubber, and behind rubber provided measurements on the temporal and spatial pressure distribution. A high-speed digital movie camera captured the bullet-armor interaction and provided the wave motion of the soft body armor.

Figure 4 shows the measured impact forces and calculated impulses for three tests, where three types of soft body armor were impacted at different speeds. Main loading durations were between 1.5 to 2 milliseconds. Peak impact forces were between 3 to 7 kilo Newtons. The backing material used for these tests was one inch of soft tissue simulating a rubber plate on top of a one inch D40 rubber plate. Other configurations of backing rubbers were also tried.



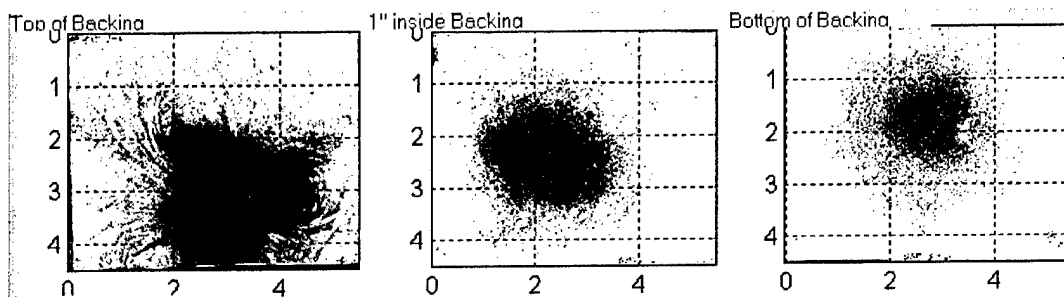
**Figure 4. Behind soft body armor impact force**

Figure 5 shows the measured impact forces and calculated impulses for hard body armors tested. Force measurements indicated that maximum capacity (range) of force gauge was reached. Therefore, a new force gauge that has higher range and natural frequency was obtained and installed in the later version of ATM. Main loading durations are shorter than in behind soft armor impacts. Peak impact forces and impulses were significantly higher than in soft body armor impacts.



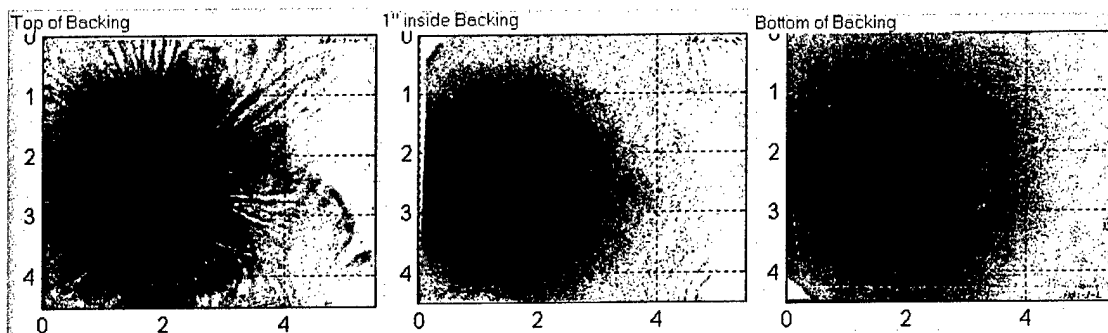
**Figure 5. Behind hard body armor impact force**

Figure 6 shows the spatial distribution of behind soft body armor impact forces at the top of the backing material, one inch behind the backing material, and at the bottom of the backing material respectively. Right underneath the impact location was an area that matched the size of the deformed bullet (0.8 inch in diameter). Usually 3-9 plies of fiber sheets were broken in this zone. Surrounding it was an area 2 inches in diameter where the ballistic fiber underwent significant plastic deformation. Further away from the impact location is a zone 3 to 4 inches in diameter where fibers were clearly stretched. Fuji film pictures inside and beneath the backing material also indicated that impact force was distributed to an area about 3 inches in diameter.



**Figure 6. Spatial distribution of behind soft armor pressure**

The spatial distribution of behind hard armor force is shown in Figure 7. Right underneath the impact location was an area that matched the size of a fragmented rifle bullet (0.8 inch in diameter). Surrounding it was an area that matched the size of a fractured ceramic conoid (2 inches in diameter). The zone where the ballistic fiber in the backing of the soft armor underwent significant plastic deformation was about 3 to 4 inches in diameter. Total area of force distribution is over 5 inches in diameter, which indicated that hard armor spread the impact load to a much larger area than the soft body armor. Fuji film pictures inside and beneath the backing material also indicated that impact force was distributed to an area above inches in diameter.



**Figure 7. Spatial distribution of behind hard armor pressure**



Pictures of damaged armor and high-speed movie snapshots are given in **Figure 8**. In order to further interpret the test results, a three-dimensional finite element model (FEM) was used to simulate the interaction among the bullet, armor, and backing materials. The bullet was modeled as an elastic-plastic metal material; the armor as an elastic-plastic composite material; and the backing as rubbery materials. The numerical simulations from the FEM with the sensor measurements and high-speed movies from the live fire tests were compared (**Figure 8**). Major findings from the testing and simulation are summarized as follow:

- ? The magnitude and duration of impacts matched well with the measurements. The duration of impacts between bullet and armor was less than one or two milliseconds, while the duration of impacts between the armor and backing materials was much longer, although the actual value depended on the velocity of the bullet and the configuration of the armor and the backing material.

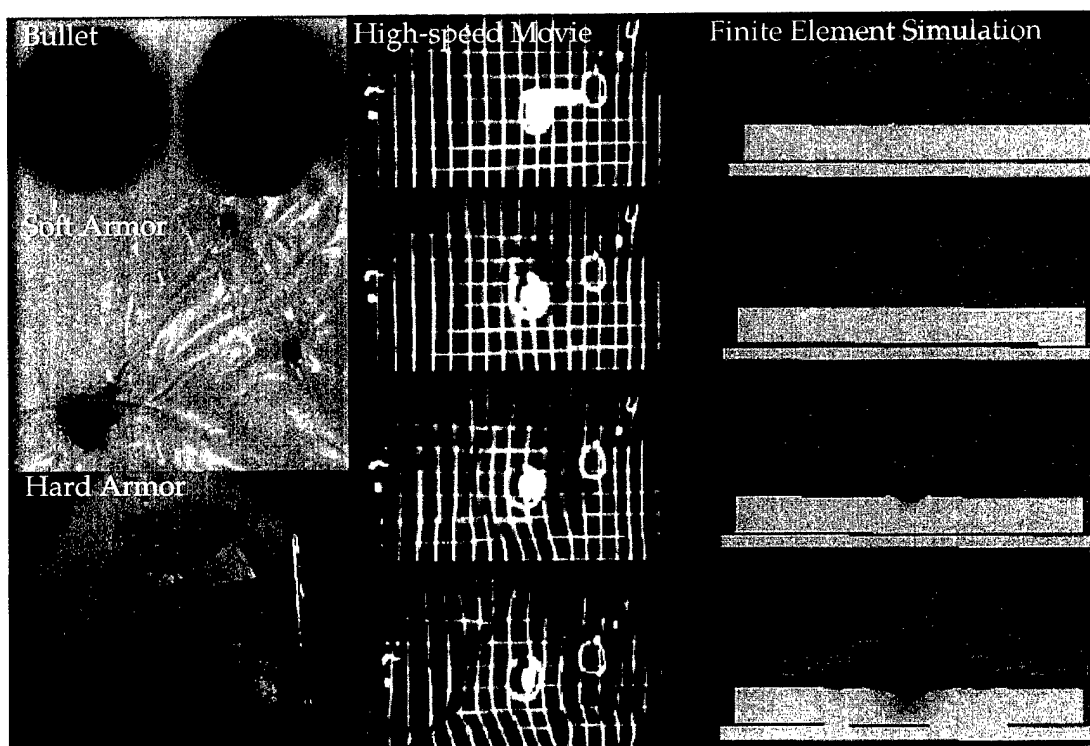


**Figure 8. Pictures from live fire test**

- ? Simulated behind armor pressure distribution and wave propagation also matched very well with the sensor measurements and high-speed movie records.
- ? The main damage mechanism for bullets is plastic deformation. For soft armor there are two distinct loading modes: shearing and tension. At certain bullet velocities, shearing mode dominates and penetration occurs. For hard armor, smeared cracking is the main mechanism.

- ? A soft armor prevents injury by spreading the momentum and energy of the impacting bullet to a larger area over the armor. Thus more mass is involved and the impacting velocity is decreased. Although the longitudinal wave speed of composite armor material is very fast, usually above 5000 meters per second, the speed at which the momentum and energy are distributed over the armor is much slower, usually much less than 1000 meters per second. This speed is predominantly affected by the stress-strain relationship of armor material.
- ? A ceramic hard armor prevents injury by blunting the high-speed rifle bullet and creating a smashed cracking zone. The bullet is usually fragmented during the process and energy is dissipated. This smashed zone, which has a much higher mass and lower velocity than the original bullet, then hits the soft armor on the back and further distributes the energy over a larger area.

The live fire test demonstrated that the armors were functioning in the same way as observed in previous animal studies where animals were impacted wearing armor. In addition, the damage of bullet and armor were also similar. This means the bullet-armor-ATM interaction is similar to bullet-armor-body interaction.

### **Impactor and Launcher Development**

The BBA impact characteristics determined from the live fire test was used to develop impactors that simulate behind soft body armor impacts. The impactor, as shown in Figure 9, is made up of a front impact plate and a base fixture. A high-shock accelerometer was mounted on the base. Special attention was paid to provide strain relief to both the sensor and the cable attached to it so that the sensor can survive the impact. Parameters, including the mass, impact plate area and shape, and impact velocity, was adjusted to match the real BBA impacts. The principle of determining the parameters is, compared with a real BBA impact, the impactor has to have: 1) similar impact area, 2) same momentum as the bullet, and 3) less kinetic energy than that of a bullet (energy dissipated due to damage of bullet and armor).

In order to deliver the impactor, a special launcher was developed (Figure 9). The launcher includes a piston sitting inside the launching barrel. The tip of the piston sticks outside the barrel and can accommodate the base of the impactor. The piston is driven by high-pressure helium gas until the end of the piston is stopped by the barrel. At that time, the impactor that has been accelerated to the desired velocity along with the piston, will free fly until it hits the target. Special attention was paid to the shock absorption at the end of the barrel so that the piston does not break due to its impact with the barrel. A net frame was also built to catch the

impactor during rebound. This is both for safety concerns and avoiding sensor damage during its rebound from the target.

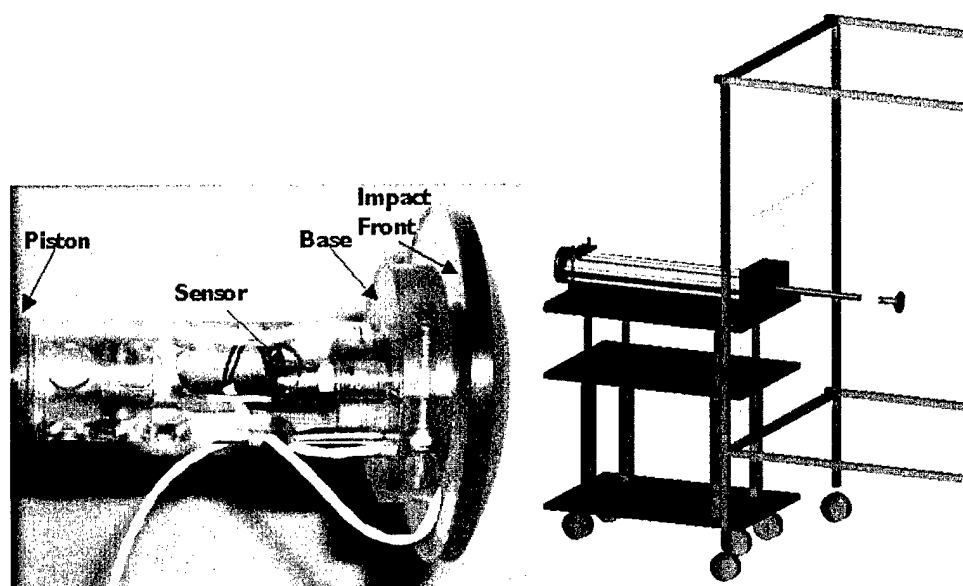


Figure 9. Impactor and Launcher

#### Quantification of Impactor -- Impactor on ATM Test

In order to verify if the impactor simulates the BBA impact, tests were conducted using the developed impactor to impact the ATM. Two tests with impact velocities of 34 and 43 m/s were conducted. The ATM measurements were compared with those obtained in live fire tests, as given in Figure 10. Results indicated that the magnitude and duration of the impulse delivered to ATM at 43 m/s matched very well with the live fire test of level II armor hit by the bullet at 361.5 m/s. This validated the concept of using the impactor to simulate actual BBA impact loads.

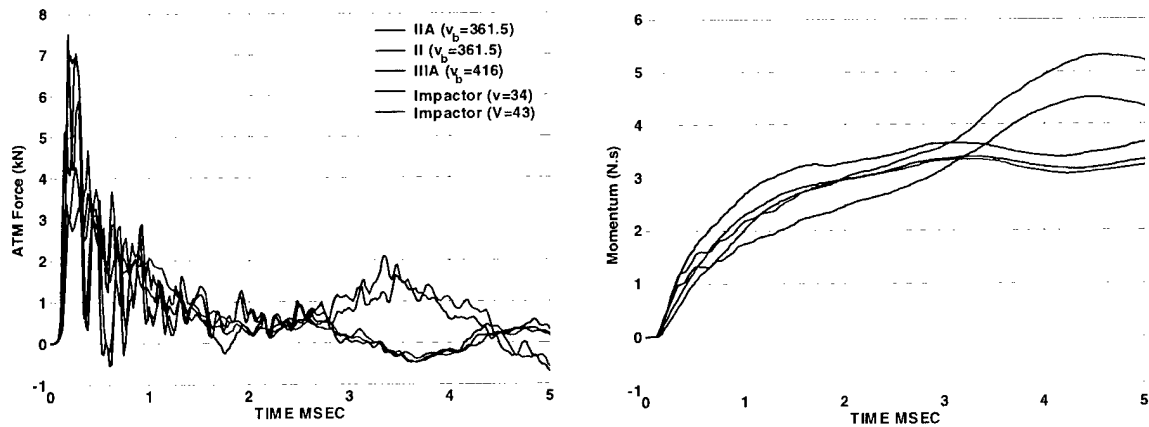


Figure 10. Comparison of Impactor-on-ATM measurements with live fire test results

### Numerical Model of ATM and Load Conversion Model

The ATM gives measured force underneath the rubber layers, instead of the BBA load. Therefore, the measurement has to be converted into the actual BBA impact characteristics. This has to be done in two steps: first a numerical model is needed to estimate the ATM measurement given the BBA impact force; and second a numerical algorithm is needed to solve the problem inversely so that given the ATM measurement, the BBA impact force can be estimated.

In order to develop a finite element model of the ATM, model parameters, most importantly those related to the rubber material properties, have to be estimated from laboratory tests. Tests were conducted for force gauge and Tekscan by applying a given impact force on the sensor and measuring sensor measurements. The sensors were then calibrated using a transfer function method. To determine rubber material parameters, a hemisphere instrumented with accelerometer was dropped onto the rubber target at various heights (Figure 11). The impact force and rubber deformation were estimated from the acceleration measurement, from which the hysteresis loops was calculated. The relaxation function of the rubber were calculated using approximate Hertz model as  $G(t) = 0.25F/(R\delta^3)^{0.5}$ .

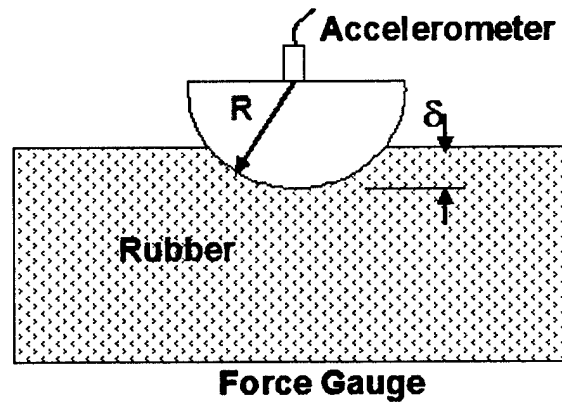


Figure 11. Laboratory hemisphere drop test

Figure 12 gives the impact force measurement and calculated rubber surface deformation for the drop tests. Two rubber configurations (a one-inch D40 rubber and a combination of one-inch soft rubber and one-inch D40 rubber), and three drop heights (2, 3 and 4 feet) were tested. Each configuration was tested three times. The test data indicated that soft tissue simulating rubber was softer than D40 rubber and led to lower impact force but longer impact duration. Figure 13 gives the deformation versus load curves for the rubbers tested. Both soft rubber and D40 rubber showed different loading and unloading phases and distinct hysteretic loops. The relaxation functions of the shear modulus are also given in Figure 13. The results are consistent for each rubber, indicating the accuracy of the method to determine the rubber viscoelastic parameters.

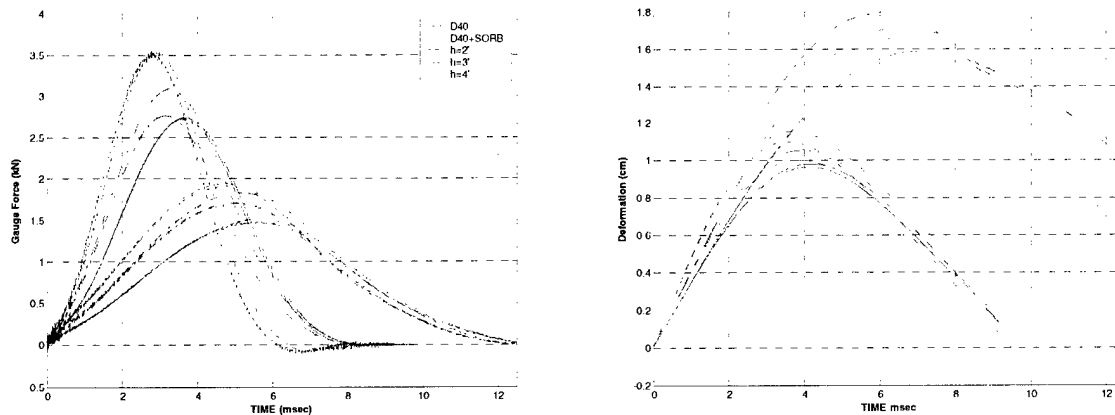
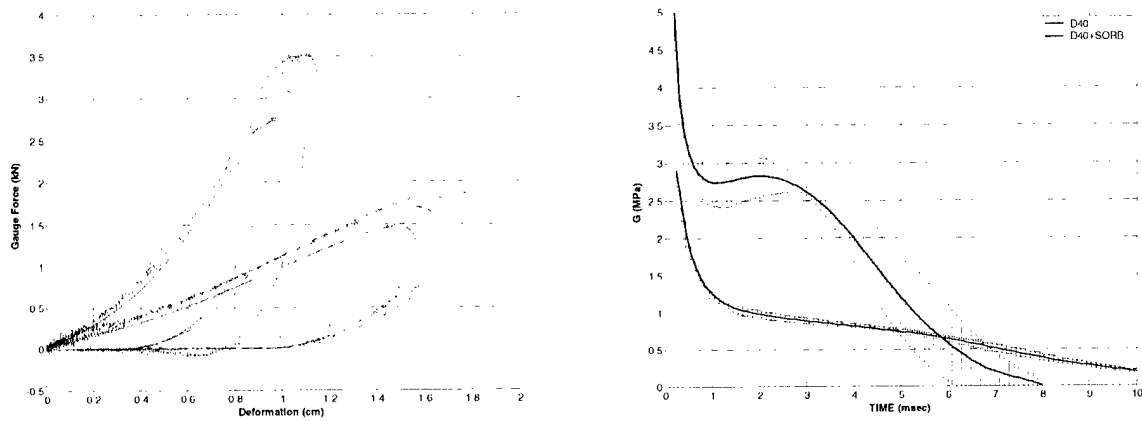
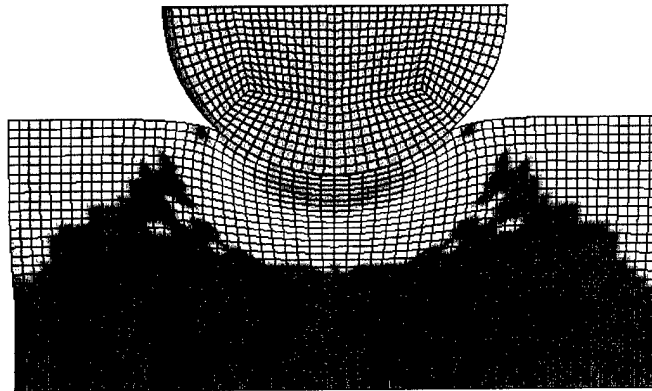


Figure 12. Impact force and deformation from hemisphere drop test



**Figure 13. Hysteresis and relaxation function of the rubber**

To determine the material parameters of the rubbers, finite element simulations were conducted to simulate the tests (Figure 14) under simulation results that matched the experiment measurement. The material model used for the rubbers was a hyperelastic rubber model (Orgen model) with linear viscoelasticity represented by Prony series. The determined material parameters are given in Table 2.



**Figure 14. FEM simulation of drop test**

**Table 2. Determined Parameters for Rubber Materials**

|                        | <b>D40</b> |           | <b>Soft Rubber</b> |           |
|------------------------|------------|-----------|--------------------|-----------|
| <b>Hyperelasticity</b> | $\mu$      | $\alpha$  | $\mu$              | $\alpha$  |
| i=1                    | 0.20       | 1.25      | 0.2                | 1.0       |
| <b>Viscoelasticity</b> | $G_i$      | $\beta_i$ | $G_i$              | $\beta_i$ |
| i=1                    | 0.15       | 3000      | 0.10               | 3000      |
| i=2                    | 0.20       | 2000      | 0.05               | 2000      |
| i=3                    | 0.40       | 1000      | 0.20               | 1000      |
| i=4                    | 0.10       | 500       | 0.10               | 500       |
| i=5                    | 0.15       | 250       | 0.15               | 250       |
| i=6                    | 0.30       | 0         | 0.02               | 0         |

To validate the model, tests were conducted using an instrumented impactor (details given in the next section) that simulates the BBA impacts (details given in the following sections) to impact the ATM (Figure 15). The speed of the impact was measured and was used to drive the FEM. The ATM measurement was compared with the model prediction. The model predicted reasonably well the magnitude and the duration of the impulse delivered to the ATM both at the top of the rubber (Figure 16) and at the bottom of the rubber (Figure 17).

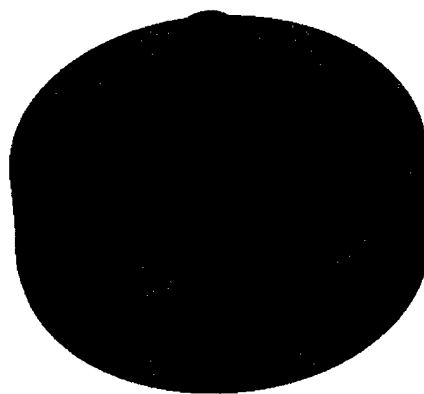


**Figure 15. FEM simulation of instrumented impactor on ATM.**

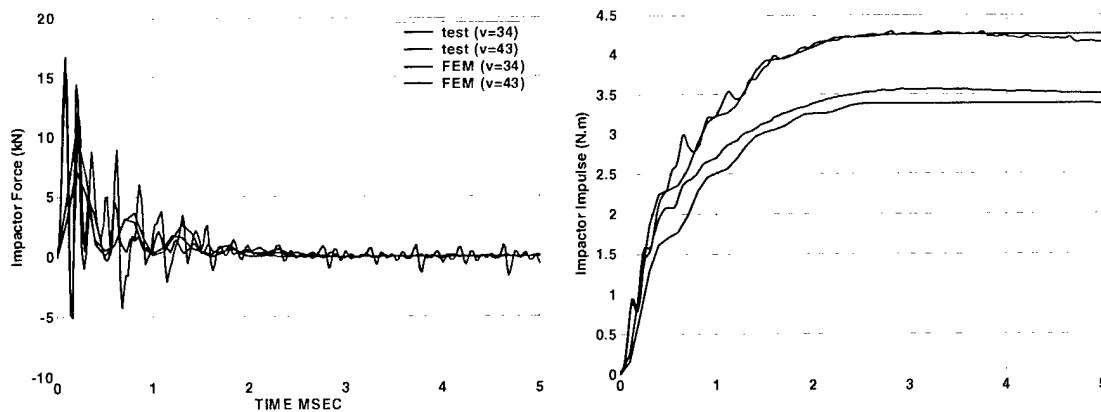


Figure 16. Comparison of FEM prediction and measurement at the top of rubber

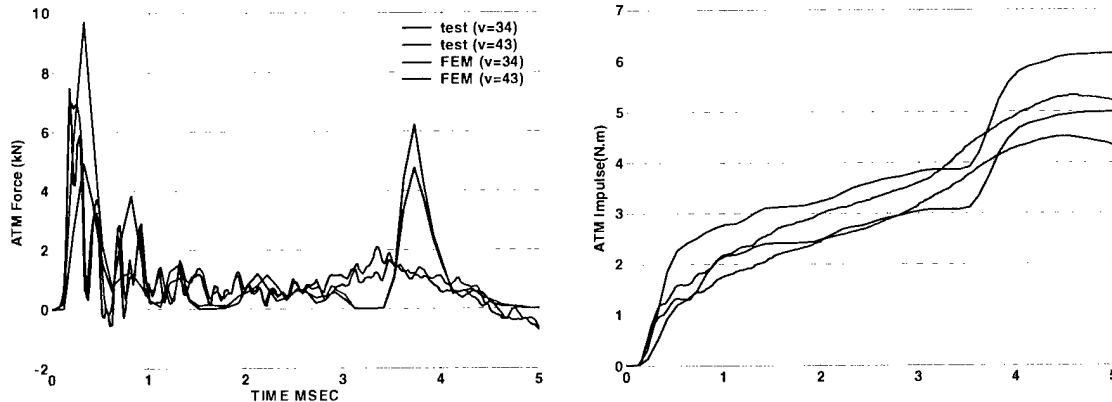


Figure 17. Comparison of FEM prediction and measurement at the bottom of rubber

### 3.2.3 Summary and Remaining Work

An ATM prototype has been developed. The live fire tests demonstrated that the ATM was durable and that the bullet-armor-ATM interaction was similar to bullet-armor-body interaction. An impactor simulating behind soft body armor impact was developed as well as the launcher to deliver it. Test results indicated that it simulated the BBA impact well; sensors mounted on the impactor were able to survive the impacts and provided good measurements. The finite element model of ATM, with parameters determined from the laboratory, was used to simulate an impact test on ATM and predicted reasonably well the ATM measurement when the impact force on ATM was measured and used to drive the model.

In the remaining work, more live fire tests using modern armors will be conducted to obtain the BBA impact characteristics; the ATM will be refined and improved; impactors will be improved and refined; the ATM FEM model will be improved to better predict the measure-



ment given the BBA force; and a load conversion model, with the ATM FEM being the core, will be developed to inversely convert the ATM measurement to the BBA impact characteristics.

### **3.3 Animal Study**

#### **3.3.1 Objective, Approach, Key Issue, and Exit Criteria**

The objective of this work area is to develop an animal model that can reproduce the significant injuries from BBA trauma and can provide useful response measurements and injury data.

Due to the restriction of firing weapons in a laboratory environment, the approach adopted here is to use impactors that simulate the BBA impact and that can be instrumented.

The key issues that have to be addressed include:

- ? Obtain the protocol that allows the impact testing on animals
- ? The animal test has to reproduce the significant injuries of BBA trauma.
- ? Use the animal response data to validate ATM response characteristics

#### **3.3.2 Summary of Progress**

##### **Animal Protocol**

An animal protocol was developed in cooperation with the researchers at the University of California at San Diego (UCSD). The animal tests will be conducted in two phases, with the first phase being exploratory using 25 animals. The first-phase protocol has been approved by the UCSD animal use committee. The approval of the protocol also required further monitoring and approval for the use of animals by the UCSD veterinarian.

The actual protocol is as follows. Pigs will be anesthetized in the UCSD/CTF laboratory, intubated (6.0-8.0 ID oral-nasal tube with inflation cuff), and a venous catheter secured in the groin for contrast administration. Animals will be kept warm using a water-controlled heating pad except during transport. An ultrasound study of the liver and spleen will be performed with ultrasound contrast. They will be transported to the CT suite (200 yards away), imaged with CT with intravenous contrast (1ml/kg), transported back to the laboratory and one impact test will be conducted. They will then be euthanized and necropsied to assess the chest wall and internal organs for injury. Anatomical data (weight, size, critical dimensions) will be collected for each animal.

The protocol also allows up to three nontrauma producing impacts, for the purpose of calibrating finite element model response prediction and determining tissue material property.

In addition, if the animal survives the traumatic impact, the protocol allows it to be transported back to the CT suite and reimaged with a second dose of 1ml/kg IV contrast. This may provide detailed information of soft tissue injury that can be compared with stress prediction from the FEM to develop injury correlation.

### **Animal Testing**

Three animal tests have been conducted thus far. In the first test, the animal was impacted by the impactor in the lower right thorax. The injuries caused by the impact included lung contusion, liver laceration, rib fractures, and mild heart lesion. The other two tests impacted the animal in the upper right thorax. Fractured ribs and lung contusions were the major injuries observed. Figure 18 shows pictures of observed injuries and snapshots of high-speed movie recordings are given in Figure 19.



**Figure 18. Some injuries observed in animal study**  
(a) Lung contusion; (b) Rib fracture; (c) Liver laceration

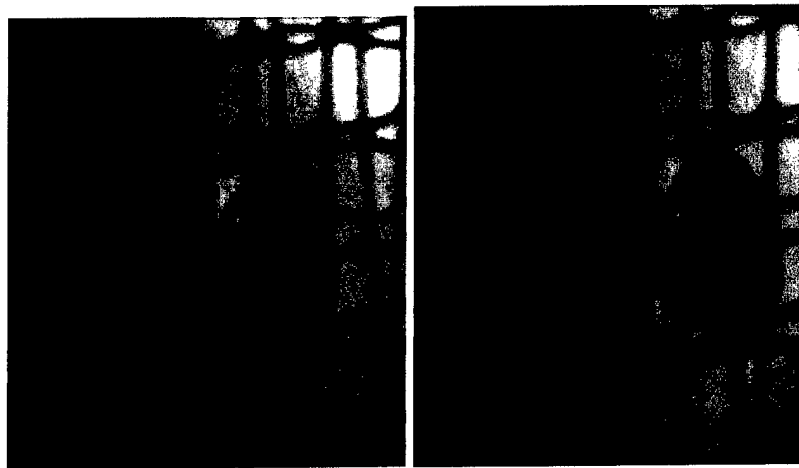


**Figure 19. High-speed movie snapshots of impactor-animal interaction.**

In each of the tests, the accelerometer mounted on the impactor survived the impact and gave good measurement. A high-speed movie camera was also used to record the impact. Impact velocity was determined and confirmed by, 1) integration of acceleration, 2) from high-speed movie recording, and 3) calculations using the free flying distance and the flight time determined from the acceleration trace. Deformation of the chest wall at the impact location was

estimated by integration of the acceleration twice over time. The impulse delivered to the chest is estimated by multiplying the impact mass by the velocity trace. Figure 20 and Figure 21 give the motion responses and force response measurements and calculations for the three animal tests. The first test impacted the animal's lower right chest at about 45 m/s. The second and the third tests impacted the animal's upper right chest at 50 and 39 m/s respectively. Despite the difference in initial velocities, the deceleration of the impact is very similar, with impactor speed reaching zero in about 1 millisecond. The peak deformation is between 1.6 to 1.8 centimeters. The main loading duration is also about 1 millisecond.

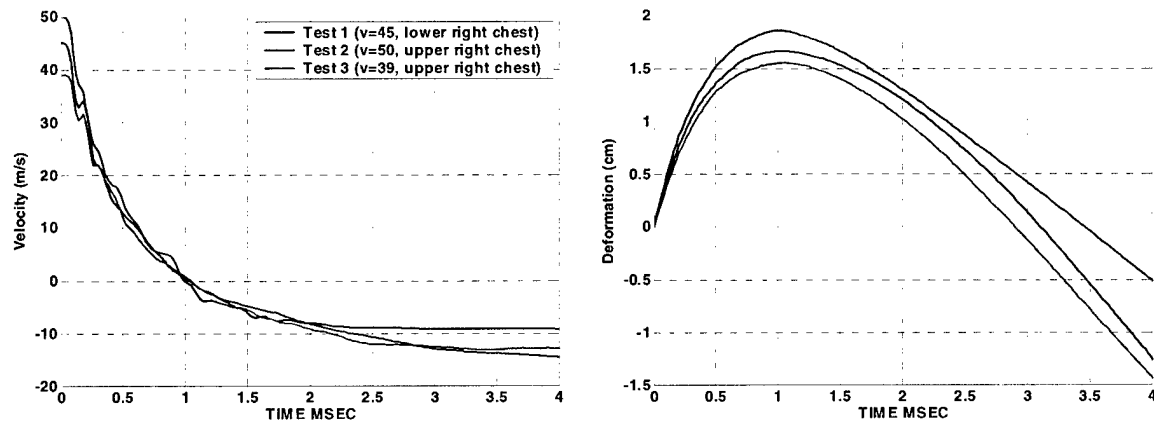


Figure 20. Measurement of velocities and deformations in animal tests

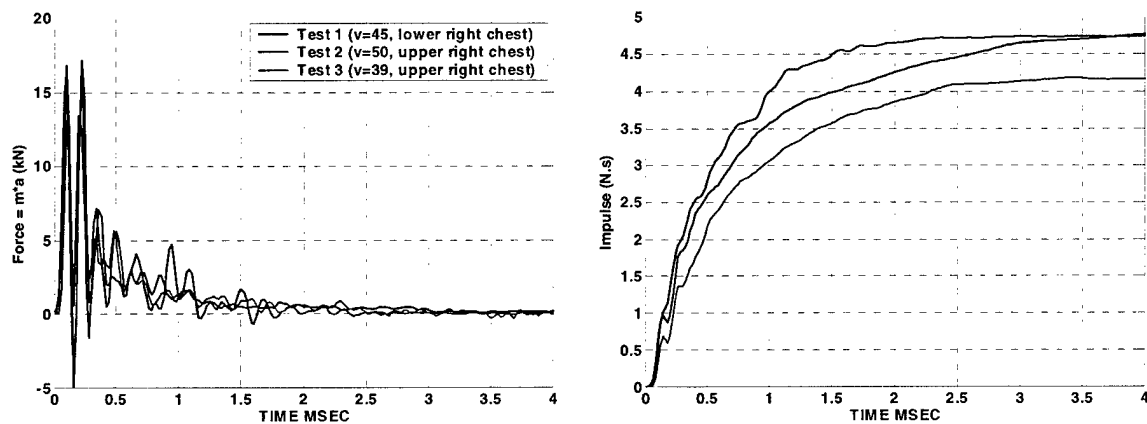


Figure 21. Measurement of impact forces and impulses in animal tests

Medical images were taken for each animal subject before the impact. A post-impact imaging was also conducted for the first animal (Figure 22), which confirmed the feasibility of using medical imaging to provide data to monitor the development of soft tissue injury due to blunt impact.

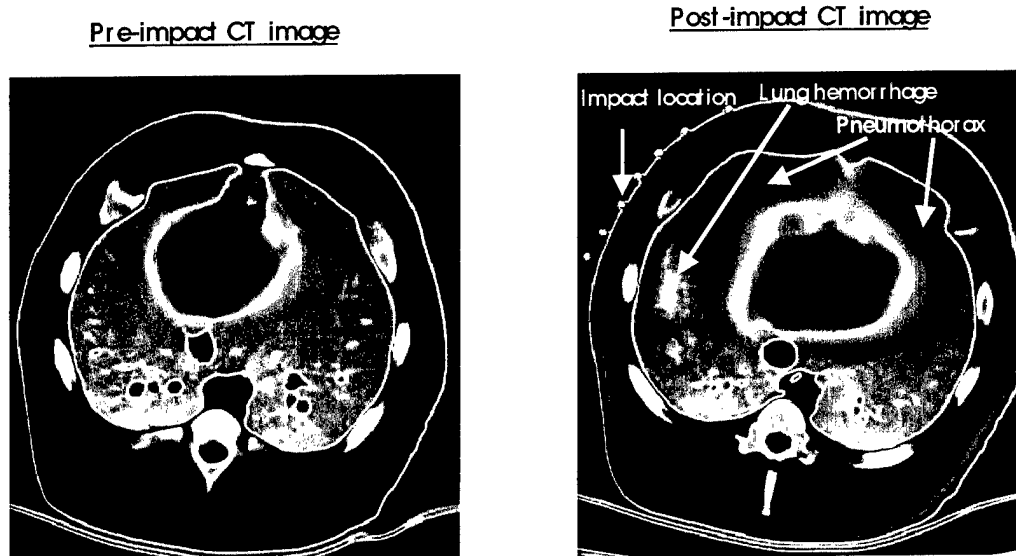


Figure 22. Pre- and post-impact CT imaging for Pig # 1 showed the feasibility of using medical imaging to study the soft tissue trauma injuries.

### Quantification of ATM Response

The response data measured in the animal study were compared with those measured in impactor-on-ATM tests. Figure 23 shows the comparison of the impulse time history and deformation time history. With the increase of impact velocity, both impulse and deformation increase. The impulse and deformation from ATM match very well with the animal response at roughly the same impact velocity. This demonstrates that the ATM tested is likely a good surrogate device to represent the body response.

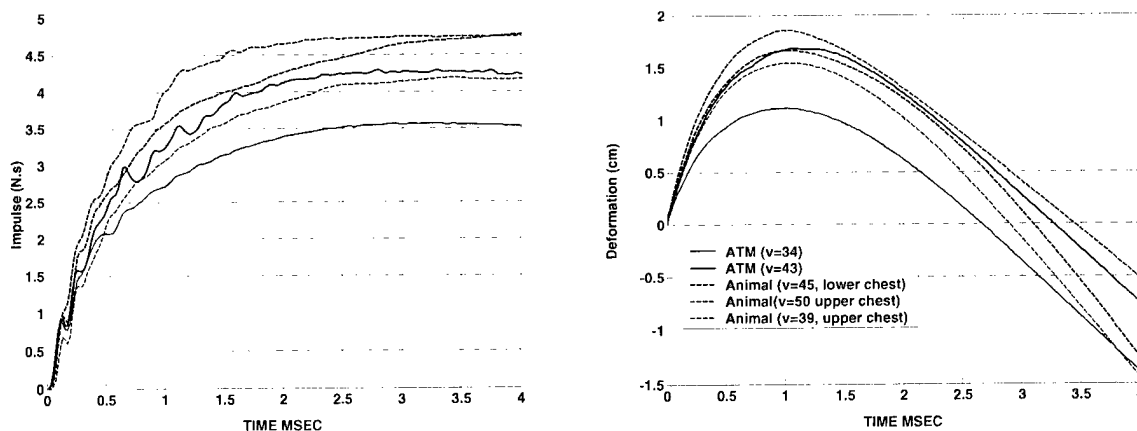


Figure 23. Comparison of animal response and ATM response characteristics.

### 3.3.3 Summary and Remaining Work

The animal study has been successful: the animal protocol was approved; three animal tests have been conducted using impactors with sensors mounted. The impactors were able to

survive the impacts and provided good measurements. Comparison of animal response data with impactor-on-ATM test data demonstrated that the ATM was likely a good surrogate device. More animal tests will be conducted in the future with varying impact parameters.

### **3.4 Animal and Human Finite Element Model**

#### **3.4.1 Objective, Approach, Key Issue, and Exit Criteria**

The objective of this task area is to provide a quantitative method for translating the load distribution measured by the ATM into an estimate of local stress needed by each of the injury correlates.

The technique approach involves:

1) Develop a procedure for generating a finite element model of individual test animal subjects. The model should resolve the specific tissues that are injured (lungs, ribs, liver, etc.), using anatomical geometry from subject-specific medical imaging;

2) Incorporate material models and parameters based on literature review and past experience. Material models that have been proposed for individual organ tissues will be the starting point for analysis. Sensitivity studies will be conducted to determine which parameters are most important to the tissue stresses;

3) Calibrate model parameters to match animal response data. It is expected that the literature values, which have been calibrated based on a different model, will need to be refined. The most sensitive parameters will be varied to determine the optimum parameters for all of the tests;

4) Generate a finite element model of man. This model will be based on medical imaging of the available human data sets;

5) Simplify the model and develop a method to scale the model. After the fidelity of the injury prediction has been demonstrated, the FEM will be simplified to produce a faster running model that retains overall injury prediction fidelity. A method will be developed to scale the model according to anatomical variation in people of different sizes.

The FEM model is judged by

- ? Comparing predicted and measured animal response (deformation and velocity) and impact force when a consistent set of material properties are used.
- ? The animal mathematical model coupled with the injury correlates is confirmed by animal injury data for different magnitudes and locations

- ? The human FEM is confirmed against available impact response data (say, Kroell test data).

### 3.4.2 Summary of Progress

#### Swine Thoracic FEM

A method for developing swine thoracic FEM based on CT images of a specific animal subject was developed. A review of previous FE modeling efforts (Deng *et al.* 2000; Masiello 1997; Lee *et al.* 1995; Kanno *et al.* 1993; Chen 1978; Sundaram *et al.* 1977; Andriacchi *et al.* 1974) was made to select a model that has the necessary details for BBA simulation but is computationally efficient. Individual organs and tissues of the animal were reconstructed to obtain the organ geometries (Figure 24). Finite element meshes were then created and assembled into the swine thoracic FEM model. The model includes ribs, spine, sternum, lungs, heart, diaphragm, skin, and chest-wall muscles (Figure 24).

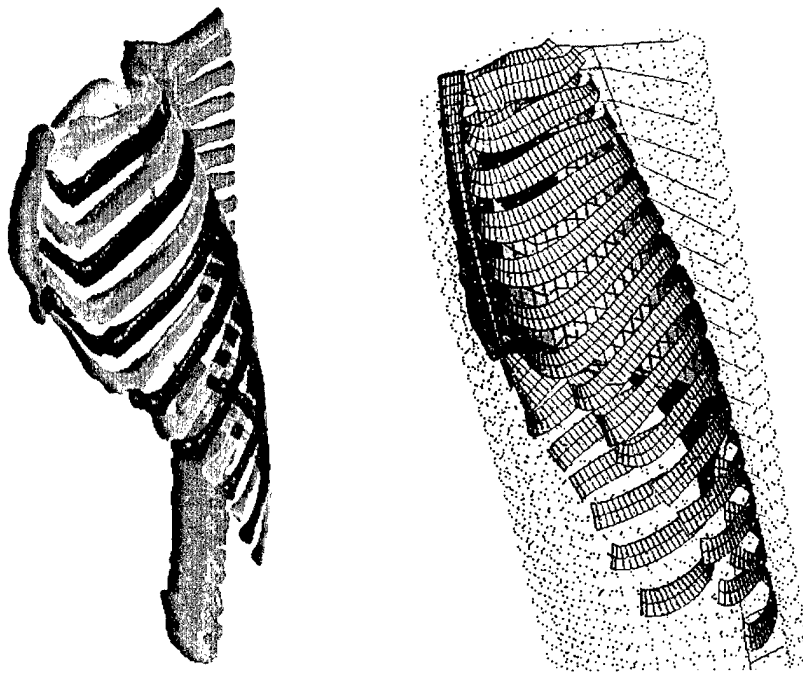


Figure 24. Constructed swine anatomy and FEM of the swine thorax.

Accurate 3D modeling of bony structure is computationally expensive. Bone has a high modulus and 3D mesh requires very small element size, which leads to small time steps in transient dynamic analysis. Special treatment was given to the rib cage in order to reduce the computational cost. Spine was simplified using the model of Patwardhan *et al.* (1990) and Gilbertson (1993). The spine was represented by a series of linear beam elements, each representing a motion segment with nodes at the vertebral body centroids. Additional beam elements were added to transfer the forces and moments to the motion segments through the

vertebral processes and the rib attachment points. The nodal coordinates were obtained from the CT images. The beam property was obtained using the method in Gilbertson (1993).

Ribs are very important in carrying the load during the impact. It is recognized that, due to the fact that bone material in ribs is inhomogeneous and the characteristic dimension of rib is small, it is extremely difficult and numerically costly to develop a detailed 3D finite model for rib. Special methods were developed to incorporate ribs into the model. First, ribs were reconstructed from CT images. The CT number was obtained for each pixel and used to determine the density of the bone (Taylor *et al.* 2002; Rho *et al.* 1995; Keyak *et al.* 1990). The elastic modulus for the pixel was then determined from the density (Choi *et al.* 1992; Goldstein *et al.* 1991; Hodgkinson *et al.* 1990; Carter *et al.* 1977). A 3D inhomogeneous finite element model was then developed for each rib. Beam formulations, based on both classical beam theory and composite beam theory (Couteau *et al.* 1998), were developed and used to create an inhomogeneous beam model that is equivalent to the 3D inhomogeneous rib. An extensive numerical study was conducted and it was concluded that the beam representation of the rib was accurate and very efficient.

Lungs, heart, skin and skeletal muscles were modeled using 3D elements. Material constitutive relationships and parameters were based on literature and previous modeling work (Fung 1993; Yamada 1970; Dunn *et al.* 1983; Weiss *et al.* 1996; Truong *et al.* 1978; Truong 1974; Carter *et al.* 2001; Farshad *et al.* 1999; Liu *et al.* 2002; Liu *et al.* 2000; Miller 2000; Miller *et al.* 1997; Silver *et al.* 2001; Miller-Young *et al.* 2002; Deng *et al.* 2000). In general, soft tissues were modeled as nearly incompressible visco-hyperelastic materials. The nonlinear elasticity parameters were selected to best fit the available test data of tissue stress-strain relationships. Viscoelasticity was dealt with by using multiple terms of Prony series with the parameters determined to best match the available relaxation data and lead to nearly constant hysteresis over the frequency ranges of interest. Details of the swine thoracic FEM development will be given in a separate report later.

Simulations of the animal test (Figure 25) were conducted using the developed swine FEM. Impact force and chest wall deformation at the impact spot were compared with the experiment data. Using the baseline material parameters, determined as previously described, led to good agreement of both the impact forces and impulses delivered to the animal chest (Figure 26) and the velocity and deformation of animal chest (Figure 27).

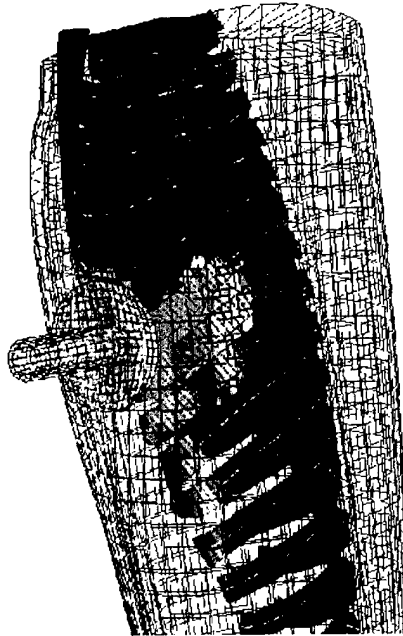


Figure 25. FEM simulation of animal test.

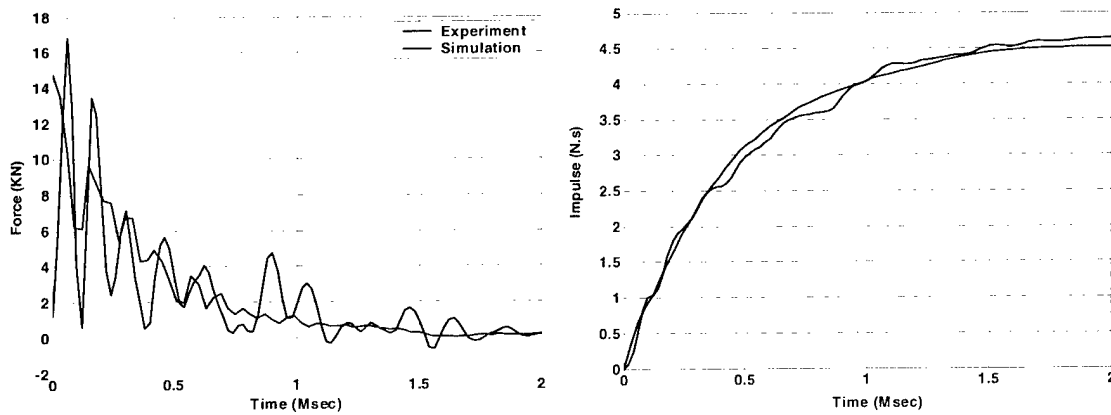


Figure 26. Comparison of FEM prediction of impact forces with animal test data

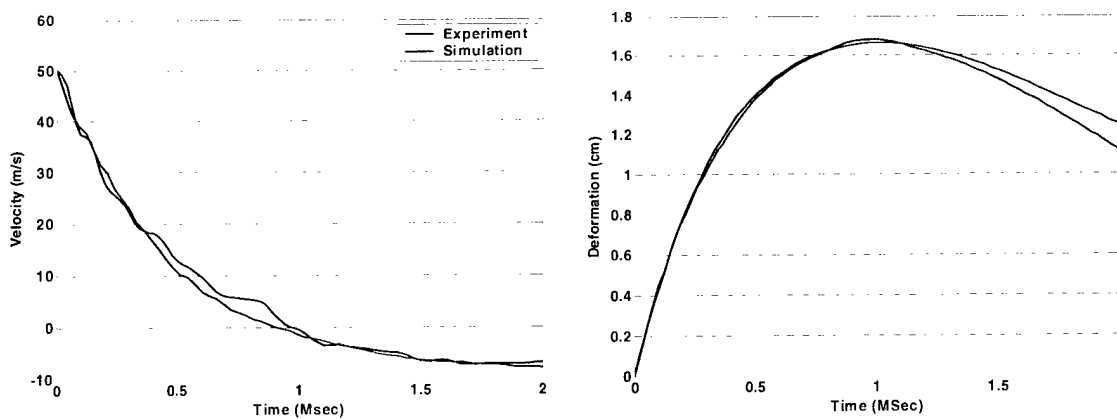


Figure 27. Comparison of FEM prediction of motion response with animal test data



## Human Thoracic FEM

Similar efforts using the same approach were also made to develop a human thoracic FEM. Geometry data of the human model came from a commercially available human anatomy data set and the Visible Man data set (Ackerman 1991; Ackerman *et al.* 2001). So far rib cage, lungs and heart have been completed (Figure 28). The skin, muscle and spine are being added.

### 3.4.3 Summary and Remaining Work

An animal thoracic FEM has been developed that has the accurate anatomy of the specific animal subjects. Baseline material properties were selected to best fit the available material data. The model was calibrated against the animal test measurement by varying model parameters. Good agreement between the simulation results and measurements was obtained. A human thoracic model is close to being finished.

In the future, swine FEM will be continuously developed and improved as more animal tests are conducted. Abdominal organs will also be added into the model. Human thoracic FEM will be completed and abdominal organs will be added. Efforts will also be made to further simplify the model and to develop methods to scale and/or morph the models for different groups of population.

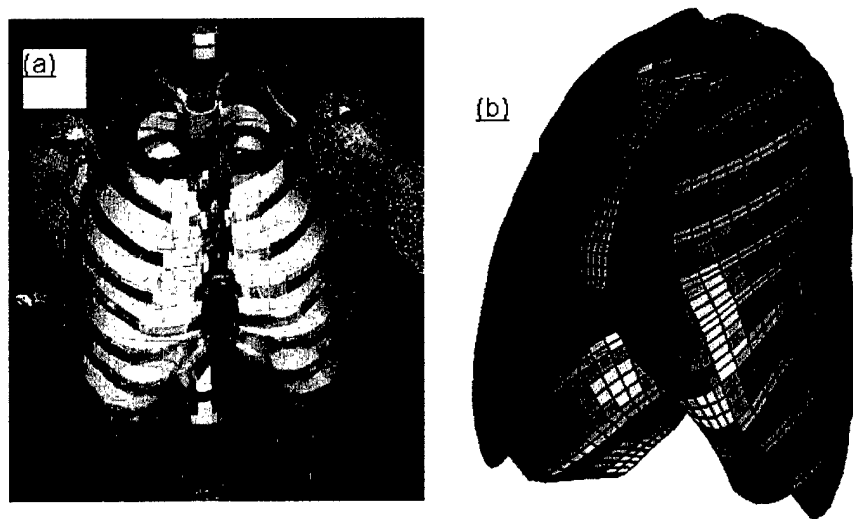


Figure 28. Human thoracic FEM

(a) A human thoracic FEM developed for car crash simulation was found not suitable for BBA impact simulation; (b) Human thoracic FEM for BBA simulation is under developed based on Visible Human Data set

### 3.5 Biomechanical Correlations for Significant Injuries

#### 3.5.1 *Objective, Approach, Key Issue, and Exit Criteria*

The objective of this task area is to produce correlations of probability or severity of injury to tissue stress for each of the significant injuries observed. Injuries to be studied include lung contusion, rib fracture, liver laceration, heart lesion, etc.

The animal FEM, calibrated for each specific test animal-impact combination, will be used to compute the appropriate tissue stress for each of the injury modes. The predicted stresses will be compared with observed injury. By conducting animal tests with varying impact parameters (area, duration, magnitude, location) that leads to different level of injuries, correlation or tolerance for each injury mode in terms of tissue stress will be developed. Existing criteria will be confirmed or refined based on these results. The correlation will be extrapolated to humans either directly or by including the difference of tissue properties among species if relevant material data become available.

Correlates will be satisfactory when they:

- Provide a clear definition of the injury progression
- Are confirmed for different impact magnitudes and locations

#### 3.5.2 *Summary of Progresses*

Since only three animal tests have been done, there is not enough data to develop injury correlation at this time. However, calibrated swine FE did predict the stress distribution that matched reasonably well with the observed injury pattern.

The locations of the maximum tensile stress of rib predicted by the model were the same as the rib fracture spots. Figure 29 shows the calculation of maximum stresses and strains of all the ribs on the impacted side from the FEM simulation of animal test number two. There were six ribs, rib R05 to R10, fractured during the test. The FEM predicted significantly higher stresses and strains for these ribs than the rest of the ribs on the same side.

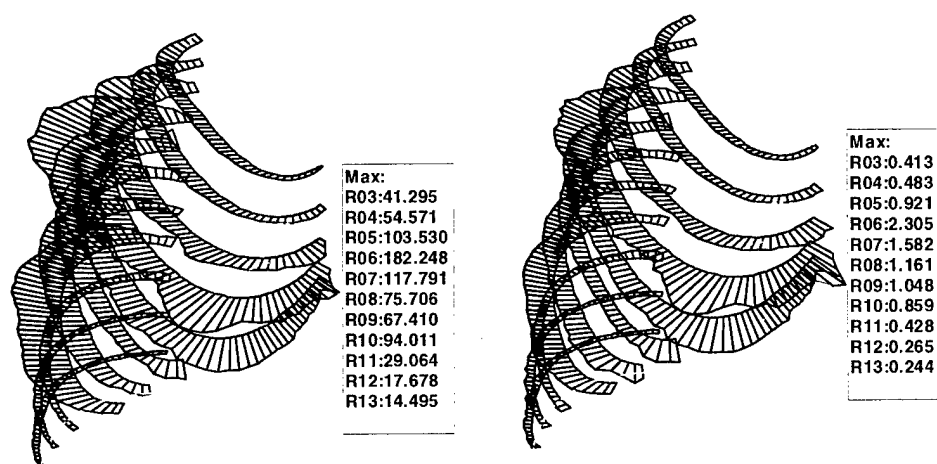


**Figure 29. Maximum rib tensile stresses and strains**

A detailed analysis of several stress and strain based quantities that may be related to rib fracture potential is given in Table 3. The approximate threshold of rib fracture is estimated within the range between the maximum value of nonfractured rib and the minimum value of the fractured rib. The ranges are listed in the last row of the table for each correlate. The results were consistent that all the correlates led to higher value for fractured ribs R06 to R10.

**Table 3. Prediction of rib fracture threshold from FEM simulation of animal test**

| Rib # | Normal Stress (Mpa) | Shear Stress (Mpa) | Normal Strain (%) | Shear Strain (%) | Coulomb Mohr (MPa) | Modified Mohr (MPa) | Hoffman Value (MPa) | Distortion Energy (MPa) |
|-------|---------------------|--------------------|-------------------|------------------|--------------------|---------------------|---------------------|-------------------------|
| R02   | 36.0                | 41.7               | 0.4               | 0.6              | 37.1               | 36.0                | 36.5                | 41.1                    |
| R03   | 41.3                | 45.5               | 0.4               | 0.7              | 42.1               | 41.3                | 41.6                | 45.0                    |
| R04   | 54.6                | 59.8               | 0.5               | 0.8              | 54.9               | 54.6                | 54.7                | 59.6                    |
| R05   | 103.5               | 116.8              | 0.9               | 1.5              | 103.9              | 103.5               | 103.7               | 116.6                   |
| R06   | 182.3               | 197.5              | 2.3               | 3.1              | 183.2              | 182.3               | 182.6               | 196.9                   |
| R07   | 117.8               | 118.8              | 1.6               | 2.1              | 118.6              | 117.8               | 118.1               | 118.3                   |
| R08   | 75.7                | 77.4               | 1.2               | 1.6              | 77.1               | 75.7                | 76.3                | 76.6                    |
| R09   | 67.4                | 71.5               | 1.1               | 1.8              | 67.8               | 67.4                | 67.6                | 71.3                    |
| R10   | 94.0                | 101.3              | 0.9               | 1.4              | 94.4               | 94.0                | 94.2                | 101.1                   |
| R11   | 29.1                | 34.7               | 0.4               | 0.7              | 33.5               | 29.1                | 31.3                | 32.2                    |
| R12   | 17.7                | 21.6               | 0.3               | 0.5              | 20.1               | 17.7                | 18.5                | 19.6                    |
| R13   | 14.5                | 21.1               | 0.2               | 0.5              | 19.6               | 14.5                | 17.2                | 18.5                    |
| R14   | 16.3                | 22.9               | 0.3               | 0.5              | 21.3               | 16.3                | 18.9                | 20.4                    |
| Range | 54.6-67.4           | 59.8-71.5          | 0.5-0.9           | 0.8-1.4          | 54.9-67.8          | 54.6-67.4           | 54.7-67.6           | 59.6-76.6               |

The predicted stress contour in the lung also matched well with the observed lung contusion (Figure 30). The peak pressure value was found to be greater than 100 kilopascals, which is the value believed to cause significant lung injury from previous research.

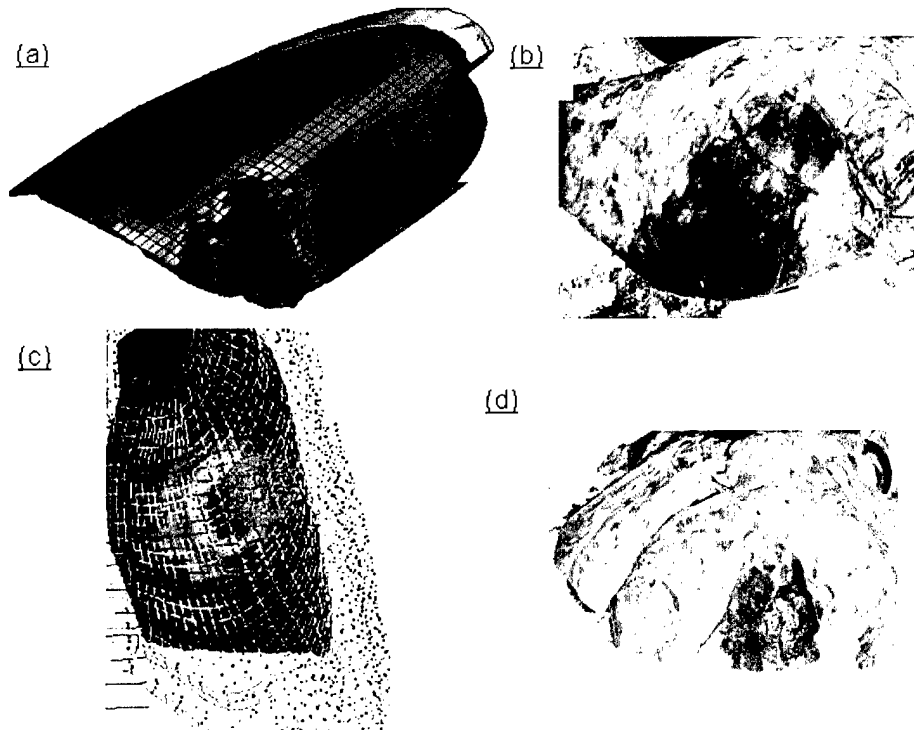


**Figure 30. Lung stress predicted by FEM and the lung contusion observed in the test**  
(a) Swine FEM simulation of impactor test; (b) Lung contusion observed in the animal study ; (c) Human FEM simulation of nonlethal weapon (NLW) impact; (d) lung injury observed from animal test of NLW

## 4. Summary

A systematic research approach was developed to conduct the project in four areas: measuring and estimating BBA impact force; using a mathematical model to predict body response; establishing a correlation between body response and injury; and using animal tests to validate body response model and injury correlations. Work has been conducted in each of these areas to address the key issues. It is concluded that the research approach adopted here is sufficient to meet the project objectives. The summary of finished work and future tasks is given in the following table.

| Key Issues  | Ans. | What we have done  | What we will do  |
|---|------|--|--|
| <b>Determine BA Force</b>   |      |  |  |
| Can we develop a durable ATM to provide measurement reliably            | Yes  | Developed an ATM that is easy to use in ballistic testing of armor and measures the special and temporal distribution of forces beneath rubber layers<br><br>Conducted live fire test using soft and hard body armors. The ATM performed well during multiple live firings.  | Further refinement and calibration of ATM<br><br>More live fire tests to characterize the BA forces  |
| Does bullet-armor-ATM function similar to bullet-armor-body interaction | Yes  | Live fire test results of bullet-armor-ATM interaction show that both soft and hard armors functioned in similar ways as they did in previous animal studies where animals wearing armor were impacted by bullets  |  |
| Can we determine BA load characteristics from ATM measurement           | Yes  | Based on laboratory calibration test, a preliminary numerical model of ATM was developed to predict the ATM measurement from input BA force<br><br>Tests using an instrumented impactor hitting ATM showed that the model prediction matched the measurement reasonably well | Further improve and calibrate the numerical model<br><br>Develop a method to solve the problem inversely, i.e., predict the BA force given the ATM measurement |

|  |        |  |  |
|--|--------|--|--|
| <b>Animal Study</b>  |        |  |  |
| Is it feasible to conduct the designed animal tests  | Yes    | Animal protocol approved<br>SBA impactor and launcher developed<br>3 animal tests conducted successfully   | SBA impactor improvement<br>HBA impactor development<br>More tests   |
| Is it valid to use an instrumented impactor in lieu of real BBA impact                         | Yes    | Same types of injuries observed as in previous animal studies where real bullet and armors were used<br><br>Similar ATM force measurement in impactor-armor-ATM and bullet-armor-ATM   |  |
| <b>Animal &amp; Human FEM</b>  |        |  |  |
| Is it feasible to develop an animal FEM that is anatomically accurate                          | Yes    | CT images obtained from animal subjects tested<br><br>Thoracic FEM developed that has the accurate anatomy   | Develop a method to automate the process<br><br>Animal abdominal FEM   |
| Can material parameters be determined for the FEM  | Yes    | Literature review of properties of main materials such as bone, skin, muscle, lung, heart. etc. gave the baseline material model and parameters<br><br>Parameters adjusted until the simulation of animal tests yielded results that matched the measured impact force and deformation | Conduct sensitivity study of the material parameters to reduce model complexity  |
| Can the model be validated   | Yes    | Simulations of animal tests conducted. Force and deformation predictions were in good agreement to the measurements  | More simulations of different animal tests   |
| Is it possible to develop a human FEM that accurately predicts the human response to BA impact | Likely | Human thoracic FEM developed based on medical imaging of visible human (anatomically accurate)<br><br>Baseline material property determined<br><br>Simulation results are qualitatively convincing   | Model further development and refinement<br><br>Human abdominal model<br><br>Study the difference between human and animal material properties |

|   |        |   |   |
|---|--------|---|---|
| How the model can be simplified to reduce computational time      | Yes    | Special formulation of ribs developed   | Sensitivity study to reduce model parameters  |
| <b>Injury correlation</b>   |        |   |   |
| Is it feasible to develop correlation of injury and tissue stress | Yes    | FEM simulation of animal test yield stress fields that match the injury patterns  | Develop correlation based on simulation and animal tests<br><br>Post-imaging, etc. to help              |
| Can the correlation developed for animal be used for human        | Likely | Through FEM, geometrical effect due to anatomical difference has already been accounted for<br><br>At tissue level, which these correlation are based, it might be able to assume that difference in animal and human tissues can be ignored<br><br>Research in material properties and strength might provide data for extrapolating the correlation from animal to human<br><br>The correlation may be validated or calibrated through the examination and simulation of the actual BA injury cases | Look into these areas   |
| Can the correlation be applied for the general population         | Likely | Anatomical difference can be resolved by scaling/morphing the FEM for different representative population groups<br><br>Difference in material property--see answers to last question   | Method of scaling and morphing FEM<br><br>Look into the variation in material property among population |

## 5. References

- Ackerman, M. J. The Visible Human Project. *J.Biocommun.* 18[2], 14. 91.
- Ackerman, M. J., Yoo, T., and Jenkins, D. From data to knowledge—the Visible Human Project continues. *Medinfo.* 10[Pt 2], 887-890. 01.
- Andriacchi, T., Schultz, A., Belytschko, T., and Galante, J. A model for studies of mechanical interactions between the human spine and rib cage. *J Biomech* 7[6], 497-507. 74.
- Behiri, J. C. and Bonfield, W. Fracture mechanics of bone--the effects of density, specimen thickness and crack velocity on longitudinal fracture. *J Biomech* 17[1], 25-34. 84.
- Carter, D. R. and Hayes, W. C. Compact bone fatigue damage: a microscopic examination. *Clin.Orthop.* [127], 265-274. 77.
- Carter, F. J., Frank, T. G., Davies, P. J., McLean, D., and Cuschieri, A. Measurements and modelling of the compliance of human and porcine organs. *Med.Image Anal.* 5[4], 231-236. 01.
- Chen, P. H. Finite element dynamic structural model of the human thorax for chest impact response and injury studies. *Aviat Space Environ Med* 49[1 Pt. 2], 143-9. 78.
- Choi, K. and Goldstein, S. A. A comparison of the fatigue behavior of human trabecular and cortical bone tissue. *J.Biomech.* 25[12], 1371-1381. 92.
- Cooper, G. J., Townend, D. J., Cater, S. R., and Pearce, B. P. The role of stress waves in thoracic visceral injury from blast loading: modification of stress transmission by foams and high-density materials. *J Biomech* 24[5], 273-85. 91.
- Couteau, B., Hobatho, M. C., Darmana, R., Brignola, J. C., and Arlaud, J. Y. Finite element modelling of the vibrational behaviour of the human femur using CT-based individualized geometrical and material properties. *J Biomech* 31[4], 383-6. 98.
- Cunniff, Philip M. Analysis of the system effects in woven fabrics under ballistic impact. *Textile Research Journal* 62, 495-509. 92.
- Currey, J. D. Changes in the impact energy absorption of bone with age. *J.Biomech.* 12[6], 459-469. 79.



- Currey, J. D. Physical characteristics affecting the tensile failure properties of compact bone. J.Biomech. 23[8], 837-844. 90.
- Deng, Yih-Charng and Chang, Fred. Development of a finite element human throat model. F8B. 00. GM North America Car Group.
- Dunn, M. G. and Silver, F. H. Viscoelastic behavior of human connective tissues: relative contribution of viscous and elastic components. Connect Tissue Res 12[1], 59-70. 83.
- Elsayed, N. M. Toxicology of blast overpressure. Toxicology 121[1], 1-15. 97.
- Farshad, M., Barbezat, M., Flueller, P., Schmidlin, F., Graber, P., and Niederer, P. Material characterization of the pig kidney in relation with the biomechanical analysis of renal trauma. J.Biomech. 32[4], 417-425. 99.
- Fung, Y. C. Biomechanics Mechanical Properties of Living Tissues. Second, 256. 93. Springer.
- Fung, Y. C. and Yen, M. R. Characterization and Modeling of Thoraco-Abdominal Response to Blast Waves, Vol. 5: Experimental Investigation of Lung Injury M. JAYCOR Final Report, May 1985. 85.
- Fung, Y. C., Yen, R. T., Tao, Z. L., and Liu, S. Q. A hypothesis on the mechanism of trauma of lung tissue subjected to impact load. J.Biomech.Eng 110[1], 50-56. 88.
- Gilbertson, Lars George. Mechanisms of fracture and biomechanics of orthoses in thoracolumbar injuries. 93.
- Goldfarb, M. A., Ciurej, T. F., Weinstein, M. A., and Metker, L. W. A Method for Soft Body Armor Evaluation: Medical Assessment. EBTR74073; ADA005575. 75. Edgewood Arsenal Aberdeen Proving Ground Md. Sponsor: Army Limited War Lab., Aberdeen Proving Ground, Md. Jan 1975. 31p. Report: EB-TR-74073.
- Goldstein, S. A., Matthews, L. S., Kuhn, J. L., and Hollister, S. J. Trabecular bone remodeling: an experimental model. J.Biomech. 24 Suppl 1, 135-150. 91.
- Goncharoff, V., Jacobs, J. E., and Cugell, D. W. Wideband acoustic transmission of human lungs. Med Biol Eng Comput 27[5], 513-9. 89.
- Gottesman, T. and Hashin, Z. Analysis of viscoelastic behaviour of bones on the basis of microstructure. J Biomech 13[2], 89-96. 80.
- Gunaratne, G. H., Rajapaksa, C. S., Bassler, K. E., Mohanty, K. K., and Wimalawansa, S. J. Model for bone strength and osteoporotic fractures. Phys.Rev.Lett. 88[6], 068101. 02.

- Haley, J. L., Alem, N. M., McEntire, B. J., and Lewis, J. A. Force Transmission through Chest Armor during the Defeat of .50-Caliber Rounds. USAARL9614; ADA304577. 96. Army Aeromedical Research Lab., Fort Rucker, AL. Feb 1996. 106p. Report: USAARL-96-14.
- Hodgskinson, R. and Currey, J. D. The effect of variation in structure on the Young's modulus of cancellous bone: a comparison of human and non-human material. Proc Inst.Mech.Eng [H.] 204[2], 115-121. 90.
- Hughes, T. A. Biomechanical Model of the Human Thorax for Impact Analysis. ADA370880. 99. Naval Postgraduate School, Monterey, CA. Sep 1999. 62p.
- Johnson, J. A., Cogbill, T. H., and Winga, E. R. Determinants of outcome after pulmonary contusion. J.Trauma 26[8], 695-697. 86.
- Jolly, J. E. Impact Analysis of a Biomechanical Model of the Human Thorax. ADA379713. 00. Naval Postgraduate School, Monterey, CA. Jun 2000. 134p.
- Jolly, J. E. and Kwon, Y. W. Computer Modeling and Simulation of Bullet Impact to the Human Thorax. NPSME00002; ADA378989. 00. Naval Postgraduate School, Monterey, CA. Jun 2000. 129p. Report: NPS-ME-00-002.
- Kamenev, Y. F and Kamenev, V. Y. Study of Characteristics of Backface Signature Blunt Trauma of the Chest and Abdomen in Experiments on Dogs. [6]. 00.
- Kanno, Yoshihisa, Jamal, Sohail, Yang, King H., and King, Albert I. Mathematical modeling of human thoracic responses with and without arms during side impact. Crashworthiness and Occupant Protection in Transportation Systems American Society of Mechanical Engineers, Applied Mechanics Division, AMD.Publ by ASME, New York, NY, USA 169, 189-203. 93.
- Keyak, J. H., Meagher, J. M., Skinner, H. B., and Mote, C. D., Jr. Automated three-dimensional finite element modelling of bone: a new method. J Biomed Eng 12[5], 389-97. 90.
- Lee, M., Kelly, D. W., and Steven, G. P. A model of spine, rib cage and pelvic responses to a specific lumbar manipulative force in relaxed subjects. J Biomech 28[11], 1403-8. 95.
- Liu, Z. and Bilston, L. On the viscoelastic character of liver tissue: experiments and modelling of the linear behaviour. Biorheology 37[3], 191-201. 00.
- Liu, Z. and Bilston, L. E. Large deformation shear properties of liver tissue. Biorheology 39[6], 735-742. 02.

- Mabry, R. L., Holcomb, J. B., Baker, A. M., Cloonan, C. C., Uhorchak, J. M., Perkins, D. E., Canfield, A. J., and Hagmann, J. H. United States Army Rangers in Somalia: an analysis of combat casualties on an urban battlefield. *J.Trauma* 49[3], 515-528. 00.
- Masiello, Paul J. A Finite Emelemt Model for Analysis of Thoracic Injury. J97-2997-05/024R1. 97. San Diego, Jaycor, Inc. 97.
- Metker, L. W., Prather, R. N., Coon, P. A., Swann, C. L., and Hopkins, C. E. A Method of Soft Body Armor Evaluation. Cardiac Testing. ARCSLTR78034; ADE410090; ADA329410. 78a. Army Armament Research and Development Command Aberdeen Proving Ground MD Chemical Systems Lab. Sponsor: Shared Bibliographic Input Experiment. Nov 1978. 36p. Report: ARCSL-TR-78034; ADE410 090.
- Metker, L. W., Prather, R. N., and Johnson, E. M. A Method for Determining Backface Signatures of Soft Body Armors. EBTR75029; ADA012797. 75b. Edgewood Arsenal Aberdeen Proving Ground Md. May 1975. 34p. Report: EB-TR-75029.
- Miller, C. E., Vanni, M. A., and Keller, B. B. Characterization of passive embryonic myocardium by quasi-linear viscoelasticity theory. *J.Biomech.* 30[9], 985-988. 97.
- Miller, K. Constitutive modelling of abdominal organs. *J.Biomech.* 33[3], 367-373. 00.
- Miller-Young, J. E., Duncan, N. A., and Baroud, G. Material properties of the human calcaneal fat pad in compression: experiment and theory. *J.Biomech.* 35[12], 1523-1531. 02.
- Montanarelli, N., Hawkins, C. E., Goldfarb, M. A., and Ciurej, T. F. Protective Garments for Public Officials. LWLCR30B73; ADA089163. 73. Army Land Warfare Lab., Aberdeen Proving Ground, MD. Aug 1973. 61p. Report: LWL-CR-30B73.
- National Institute of Justice, Office of Science and Technology. Ballistic Resistance of Personal Body Armor. 00. Washington, DC, U.S. Department of Justice, Office of Justice Program, National Institute of Justice.
- Patwardhan, A. G., Li, S. P., Gavin, T., Lorenz, M., Meade, K. P., and Zindrick, M. Orthotic stabilization of thoracolumbar injuries. A biomechanical analysis of the Jewett hyperextension orthosis. *Spine* 15[7], 654-661. 90.
- Pode, D., Landau, E. L., Lijovetzky, G., and Shapiro, A. Isolated pulmonary blast injury in rats--a new model using the extracorporeal shock-wave lithotripter. *Mil Med* 154[6], 288-93. 89.
- Pope, M. H. and Outwater, J. O. Mechanical properties of bone as a function of position and orientation. *J Biomech* 7[1], 61-6. 74.

- Prather, R. N., Swann, C. L., and Hawkins, C. E. Backface Signatures of Soft Body Armors and the Associated Trauma Effects. ARCSLTR77055; ADE400052; ADA049463. 77. Army Armament Research and Development Command Aberdeen Proving Ground Md Chemical Systems Lab. Nov 1977. 36p. Report: ARCSL-TR-77055; ADE400 052.
- Rajendran, A. M. Modeling the Impact Behavior of AD85 Ceramic Under Multi-Axial Loading. ARLTR137; ADA2658771. 93. Army Research Lab., Watertown, MA. May 1993. 45p. Report: ARL-TR-137.
- Reilly, D. T. and Burstein, A. H. The elastic and ultimate properties of compact bone tissue. J.Biomech. 8[6], 393-405. 75b.
- Reilly, D. T. and Burstein, A. H. The elastic and ultimate properties of compact bone tissue. J Biomech 8[6], 393-405. 75a.
- Reilly, G. C. and Currey, J. D. The effects of damage and microcracking on the impact strength of bone. J.Biomech. 33[3], 337-343. 00.
- Rho, J. Y., Hobatho, M. C., and Ashman, R. B. Relations of mechanical properties to density and CT numbers in human bone. Med.Eng Phys. 17[5], 347-355. 95.
- Sarron, J. C., Destombe, C., Caillou, J. P., Da Cunha, J., and Buck, K. Preliminary results of Oksbol experiment. 00a. 00a.
- Sarron, J. C., Destombe, C., Caillou, J. P., Da Cunha, J., Buck, K., Gotze, H., and Mayorga, Maria A. Physiological results of NATO BABT experiments. 00b. 00b.
- Shen, Weixin. Analysis of 2000 NATO Oksbol Behind Armor Animal Test Results. J3150-01-22-155. 01. San Diego, Jaycor Inc.
- Silver, F. H., Freeman, J. W., and DeVore, D. Viscoelastic properties of human skin and processed dermis. Skin Res.Technol. 7[1], 18-23. 01.
- Soderstrom, C. A., Carroll, A. W., and Hawkins, C. E. The Medical Assessment of a New Soft Body Armor. ARCSLTR77057; ADE410002; ADA053789. 78. Army Armament Research and Development Command Aberdeen Proving Ground Md Chemical Systems Lab. Jan 1978. 18p. Report: ARCSL-TR-77057; ADE410 002.
- Sundaram, S. H. and Feng, C. C. Finite element analysis in the human thorax. J Biomech 10[8], 505-16. 77.
- Suneson, A., Hansson, H. A., Lycke, E., and Seeman, T. Pressure wave injuries to rat dorsal root ganglion cells in culture caused by high-energy missiles. J Trauma 29[1], 10-8. 89.

- Sunshine, I. Thoracic Trauma: Analysis of 140 US Army Casualties in Vietnam from July to September 1967. EATR4358; AD866212. 70. Edgewood Arsenal, Md. Mar 1970. 29p. Report: EA-TR-4358.
- Taylor, W. R., Roland, E., Ploeg, H., Hertig, D., Klabunde, R., Warner, M. D., Hobatho, M. C., Rakotomanana, L., and Clift, S. E. Determination of orthotropic bone elastic constants using FEA and modal analysis. J.Biomech. 35[6], 767-773. 02.
- Truong, X. T. Viscoelastic wave propagation and rheologic properties of skeletal muscle. Am J Physiol 226[2], 256-64. 74.
- Truong, X. T., Jarrett, S. R., and Nguyen, M. C. A method for deriving viscoelastic modulus for skeletal muscle from transient pulse propagation. IEEE Trans Biomed Eng 25[4], 382-4. 78.
- U.S.Congress, Office of Technology Assessment. Police Body Armor Standards and Testing. Volume 1. OTAISC534; ISBN0160379873; PB92216100. 92. Office of Technology Assessment, Washington, DC. 14 Aug 1992. 59p. Report: OTA-ISC-534, ISBN-0-16-037987-3.
- Vinson, J. R. and Zukas, J. A. On the Ballistic Impact of Textile Body Armor. J Appl Mech Trans ASME 42, 263-268. 75.
- Weiss, Jeffrey A., Maker, Bradley N., and Govindjee, Sanjay. Finite element implementation of incompressible, transversely isotropic hyperelasticity. Computer Methods in Applied Mechanics & Engineering 135[1-2 Aug 15], 107-128. 96.
- Yamada, Hiroshi. Strength of Biological Materials. 297. 70. Baltimore, The Williams & Wilkins Company. Evans, F. G.
- Yen, R. T., Fung, Y. C., and Liu, S. Q. Trauma of lung due to impact load. J Biomech 21, 745-753. 88.